Genetically-encoded biosensors in plants: pathways to discovery

Ankit Walia[1], Rainer Waadt[2*], Alexander M. Jones[1]

[1] Sainsbury Laboratory, Cambridge University, Cambridge, CB2 1LR, United Kingdom; email ankit.walia@slcu.cam.ac.uk, alexander.jones@slcu.cam.ac.uk
[2] Centre for Organismal Studies, Ruprecht-Karls-Universität Heidelberg, Heidelberg, 69120, Germany; email rainer.waadt@cos.uni-heidelberg.de

[*] Equal contribution

To whom correspondence should be addressed: alexander.jones@slcu.cam.ac.uk

Keywords

Genetically encoded biosensors, live imaging, cell biology, calcium, dynamics, FRET

Abstract

Genetically encoded biosensors that directly interact with a molecule of interest were first introduced over twenty years ago with the advent of fusion proteins that served as fluorescent indicators for calcium ions in solution. Since then the technology has matured into a diverse array of biosensors that have been deployed to improve our spatiotemporal understanding of molecules, like calcium, whose dynamics have profound influence on plant physiology and development. In this review, we will address several types of biosensors with a focus on genetically encoded calcium indicators that are today the most diverse and advanced group of genetically encoded biosensors. We will then consider the discoveries in plant biology made using biosensors for calcium, pH, reactive oxygen species, redox conditions, primary metabolites, phytohormones, and nutrients such as zinc, phosphate, nitrate and ammonium. These discoveries were dependent on the engineering, characterization and optimization required to develop a successful biosensor and also on the methodological developments required to express, detect and analyze the readout of such biosensors *in planta*. As these steps are iterative for current biosensors and as most extant biosensors have yet to be deployed in plants, the contribution of genetically encoded biosensors to plant biology stands to grow in the future.

Introduction

In most plants, highly disparate metabolic activities occur in photosynthetic leaves, reproductive tissues, and subterranean root systems. Coordinating these activities in a dynamic environment necessitates continual mobilization of resources and information across the plant body-plan. Revealing how resources and information such as nutrients, metabolites, and signaling molecules are spatially distributed over time is thus a crucial step towards understanding how plants cope with the challenge of coordinating many cellular activities into a multicellular whole and do so in dynamic environments. Thus, there is a need to measure the levels of important molecules at physiologically relevant spatial and temporal scales and to make such measurements *in vivo*. Towards this end, many fields in which transgenesis is feasible have turned to genetically encoded fluorescent or luminescent biosensors to acquire high-resolution information with minimally invasive methodologies. Clearly a lack of such biosensors specific for a given analyte would limit a biosensing approach, but an ever-growing array of biosensors is available (144) many of which sense analytes relevant in plant biology.

Definition of Biosensors

'Biosensor' is a general term applied to many technologies that describes a molecule, organism, or device in a biological context that couples the sensing of a specific molecule of interest (analyte) or biological process to the emission of a quantifiable signal (6; 144; 161). The term 'bio' can imply a biological component of the biosensor or simply that it is incorporated into a biological system (6; 144). Idealized requirements for a 'sensor' are that it: 1) is highly selective for a specific analyte or biological process, 2) enables a quantitative readout overbiologically meaningful spatial, temporal, and concentration ranges, 3) exhibits a high signal-to-noise ratio and 4) does not perturb the biological process that it measures or the biological system in which it is integrated (144; 161; 198). A broad treatment of advances in analytic techniques including mass-spectrometry as well as ectopic and genetically encoded biosensors was recently published with a focus on the plant hormones (142). In this article we mainly focus on genetically encoded fluorescent biosensors and the latest achievements in plants using such biosensors.

Genetically Encoded Fluorescent Biosensor Types

Genetically encoded fluorescent biosensors generally consist of a sensory module coupled to fluorescent proteins (FPs) that are detected by fluorescence microscopy (161). Based on their biochemical properties and requirements for interactions with the cellular environment, genetically encoded fluorescent biosensors are categorized into indirect, typically irreversible biosensors that require additional cellular components to report on an analyte and direct, typically reversible biosensors that function independently of the cellular environment (108; 187). According to this definition, a recombinant direct biosensor can also monitor analyte concentration changes *in vitro*, while an indirect reporter cannot. Examples for indirect reporters are transcription-, degradation-, and translocation-based reporters or reporters that consist of more than one molecule. The first direct biosensors were developed to monitor cellular [Ca^{2+}] two decades ago (Miyawaki et al., 1997 - 9278050; Persechini et al., 1997 - 9330791).

Genetically encoded fluorescent biosensors are further categorized based on the properties of their sensory module and attached FPs. If the FP by itself senses the analyte, it can be considered an 'intrinsic' biosensor (144), whereas a chimera of FPs fused to a sensory module that is derived from another protein or proteins (144) is considered an 'extrinsic' biosensor. A sensory module is not necessarily a polypeptide sequence, but could also be encoded in a nucleotide sequence, for example in transcriptional reporters.

Another categorization of genetically encoded fluorescent biosensors is based on the number of incorporated FPs and whether the fluorescent readout is intensiometric or ratiometric. Single-FP biosensors are generally intensiometric with one excitation (Ex) and one emission (Em) maximum. However, single-FP biosensors can also be ratiometric when the FP has two excitation wavelengths that respond differentially to an analyte, for example the pH-sensitive ratiometric pHluorin (121) and redox-sensitive roGFPs (72). Alternatively, singe-FP ratiometric biosensors can exhibit two emission readouts that respond differentially to an analyte (73; 205). Two-FP biosensors also enable a ratiometric readout when the two FPs respond differentially to an analyte (62) or, as in Förster Resonance Energy Transfer (FRET)-based biosensors, when the two

FPs form a FRET pair and the amount of energy transfer responds to an analyte. FRET-based biosensors have typically harbored a cyan FP and yellow FP variant that function as a FRET-pair with a ratiometric readout calculated from ($Ex_{CFP}Em_{YFP}$)/($Ex_{CFP}Em_{CFP}$) (Okumoto et al., 2012 - 22404462; Uslu and Grossmann, 2016 - 26802805). Recently, a new type of ratiometric genetically encoded fluorescent biosensor has been designed based on dimerization-dependent FP (ddFP) exchange (5; 50). In the following, we will describe the principles of different genetically encoded fluorescent biosensors types in more detail and give an overview of what we learned from biosensor-based approaches in plant systems.

Indirect biosensors

Synthetic or native hormone responsive promoters or promoter motifs have been successfully used as an indirect readout for the hormone signaling strength *in vivo* (193; 198). For example, the synthetic *DR5* and *DR5v2* promoters driving β-glucuronidase or fluorescent probes report on the transcriptional response to auxin accumulation (110; 186). These reporters have been widely and successfully used to advance our understanding of auxin signaling dynamics in plant cells during plant development and environmental responses (23; 76; 110; 147; 160; 181; 186; 198).

A similar promoter-reporter approach was used to explore dynamics of cytokinins (*TCS::GFP* and *TCSn::GFP* (22; 64; 133; 207), ethylene (*EBS::GUS* (179), and abscisic acid (53). One primary limitation of these transcriptional reporters, such as *DR5* and *TCS::GFP*, is that they report the output of the hormone signaling pathway rather than the actual hormone content within a cell. Thus, the final output can vary with changes in the components of the corresponding signaling pathway and be affected by crosstalk from other pathways. Furthermore, there is often a temporal lag between the induction of the transcriptional reporter in response to an initial signaling event, reflecting the time needed for transcription, translation, and reporter protein maturation. The time-interval can be significantly improved by using fast-folding versions of GFP (such as the YFP variant VENUS) or luciferase as reporters (65; 170). For example, *DR5::VENUS* has been used to reveal changes in auxin levels during many developmental contexts, such

as developing primordia in the shoot apical meristem (76) and stomatal development (107). Despite the caveats inherent with promoter-reporter analyses, they have nonetheless been instrumental in our understanding of many physiological and developmental processes upstream and downstream of plant hormone distributions.

Fluorescent probes fused to signaling components can also be used as biosensors. Because their dynamics being tracked, e.g. localization or protein degradation, does not involve/require *de novo* transcription and translation, these reporters can exhibit improved temporal resolution and reduced potential for crosstalk from other signaling pathways compared with transcriptional reporters. For example, changes in BZR1-CFP localization have been used to reveal spatiotemporal brassinosteroid signaling in Arabidopsis roots and hypocotyls (32; 154). The localization of NIN-Like Protein7 (NLP7-GFP) is regulated by nitrate through a nuclear retention mechanism in Arabidopsis and thus can report indirectly on nitrate levels (116). Dynamics of phospholipids that play an important role in plant development as well as mediating abiotic and biotic stress responses (135) have also been monitored through localization based fluorescent probes (176; 188; 189)

Protein degradation-based reporters have also been widely used in plants, starting with GFP-DELLA fusion proteins whose stability is responsive to the phytohormone gibberellin (136). This signaling event has been used to indirectly monitor GA levels through tracking the fluorescence of GFP-RGA fusion protein (1; 49; 175). Although GFP-RGA has been observed to be stabilized compared with endogenous and untagged AtRGA (52), GA-induced cell elongation in hypocotyl cells was preceded by reduction in GFP-RGA levels (164), and an increase in GFP-RGA levels was observed in the hypocotyls during photomorphogenesis (2), where light-induced signals inhibit GA and hypocotyl growth.

In the field of auxin biology, a major advance was made where a novel biosensor, DII-VENUS, was developed in which the DII-VENUS reporter system was coupled with the degron motif of AtIAA28 (29). The DII-VENUS biosensor fluorescence levels are inversely correlated to endogenous auxin levels, and the biosensor has been used to map auxin distribution with cellular resolution during various developmental processes

(14; 15; 29; 107). A Jas9-VENUS biosensor that is degraded in the presence of JA was used to map local changes in JA levels in Arabidopsis roots and revealed two distinct phases of JA accumulation in the root upon wounding of cotyledons (105). Whereas GFP-RGA, DII-VENUS, and Jas9-VENUS are intensiometric degradation-based reporters, a ratiometric version of DII-VENUS was developed in which plants express both, the auxin sensitive DII-VENUS and a stable mDII-tdTomato (110). This R2D2 biosensor has been applied to indirectly measure auxin levels during seed development (56) and root elongation (16). Another ratiometric degradation-based biosensor, StrigoQuant, was engineered by linking AtSMXL6 with a firefly luciferase (FF) to monitor the strigolactone (SL) sensitive degradation of AtSMXL6. Inclusion of a normalization element in renilla luciferase (REN) that is not SL sensitive was used to allow a ratiometric readout. In StrigoQuant, both SM-FF and REN were engineered on a single construct separated by a self-processing 2A peptide that allowed for co-translation and cleavage from a single transcript (162). Arabidopsis protoplasts transiently expressing StrigoQuant were used to monitor the changes in ratio upon treatment with synthetic strigol-like SL analog (*rac*-GR24) as well as providing quantitative insights into the stereochemistry of strigolactone perception that has relevance at the level of receptor complex formation and initiation of SL signaling cascade.

Direct intrinsic biosensors

Intrinsic biosensors harbor modifications within the FP to make them sensitive to an analyte (144). pH-dependent excitation and emission properties are intrinsic features of FPs (144) and several FPs were engineered to monitor cellular pH changes (21; 63). Ratiometric pHluorin/phGFP is a dual excitation (395 nm and 475 nm) and one emission (508 nm) biosensor with a pKa of 6.9 (121; 130; 165). For phGFP 395 nm excitation increases and 475 nm excitation decreases with increasing pH (121). An alternative to phGFP is Pt-GFP from the organism *Ptilosarcus gurneyi* with dual excitation (390 nm and 502 nm) and one emission (508 nm) and a pKa of 7.3 (165). Note that for Pt-GFP 390 nm excitation decreases and 502 nm excitation increases with increasing pH (165). The rather neutral pKa of phGFP and Pt-GFP suits them best for pH measurements in the cytoplasm. To monitor pH changes in a more acidic environment the dual excitation

and dual emission pH biosensor pHusion (pKa of 6) has been designed, consisting of an mRFP1-EGFP tandem FP-pair with EGFP being the pH sensitive moiety (62).

The pKa of YFP is dependent on the concentration of halide or nitrate ions and at pH 7 YFP fluorescence decreases with increasing concentrations of chloride or nitrate, making it suitable as a halide biosensor (87; 194). Based on these findings YFP-H148Q variants have been generated with improved anion sensitivities for iodide, chloride and nitrate (58). Through the fusion of chloride-sensitive YFP to the insensitive CFP a ratiometric FRET-based chloride biosensor has been developed, termed Clomeleon (101). ClopHensor (E^2GFP fused to mDsRed) is a triple excitation and dual emission biosensor in which 458 nm excitation of E^2GFP is pH-independent, 488 nm excitation of E^2GFP is pH-dependent and 543 nm excitation of mDsRed is pH- and chloride-independent, making ClopHensor suitable to assess pH and chloride concentration changes simultaneously (11).

Beyond intrinsic pH and halide sensitivity, FPs have been engineered to either enhance or introduce intrinsic sensitivity to metals (33; 155), redox conditions (rxYFP and roGFP, (72; 146), and calcium (CatchER, (182).

Direct extrinsic biosensors: Calcium Indicators as Prototypes

The possibilities for designing direct extrinsic fluorescent biosensors can be best illustrated by the development of genetically encoded calcium indicators (GECIs). The development of the first GECIs two decades ago initiated the advent of direct biosensors. Since then, more than 40 fluorescent GECIs have been described (151) and the numbers are steadily increasing (Figure 1). Therefore, fluorescent GECIs are the most advanced and widely adopted direct fluorescent biosensors.

Two early design strategies for direct GECIs continue to be widely applied. These are single-FP intensiometric biosensors (13; 138; 140) and two-FP ratiometric FRET-based biosensors (124; 153). Single-FP GECIs use FPs that are split at a certain position (between amino acids 144 and 145 for GFP) and in which their original N-terminus is re-fused to the C-terminus via a short flexible linker (13). Fusion of sensory modules to such circular permutated FPs (cpFPs) with altered FP topology can have a profound effect on the FP fluorescence. This principle has been used to design two

types of cpFP based GECIs, dependent on the insertion site of the sensory module. In Camgaroos the calcium-binding calmodulin (CaM) was inserted in between the cpFP fragments (13; 66), whereas in Pericams and GCaMPs the CaM-binding M13 fragment from myosin light-chain kinase (M13) was fused to the N-terminus, and CaM was fused to the C-terminus of the cpFP (138; 140). GCaMPs have been extensively engineered to improve their signal-to-noise ratio and calcium-binding properties (4; 39; 180; 185). However, the latest achievements based on the GCaMP design include single-FP GECIs that emit fluorescence at different wavelengths (3; 205) or that enable photoactivation/photoconversion (24; 57; 79).

Two-FP ratiometric GECIs are typically FRET-based and grouped into three different classes. These are the yellow cameleons (124), the FIP-CA indicators (153) and troponin C based biosensors (75; 115; 183). In yellow cameleons the calcium-binding CaM-M13 sensory module was inserted between N-terminal ECFP as the FRET donor and C-terminal EYFP as the FRET acceptor (124). Another configuration was used for FIP-CA indicators, in which the M13 peptide linked both FPs and CaM was located at the C-terminus (153). Cameleons and troponin C based biosensors were both committed to several rounds of improvements, including the use of cpFPs as FRET acceptor (139), a re-design of the sensory module to reduce perturbation of cellular components (148) and the modification of the CaM-M13 linker to increase their calcium affinity (80).

It is also worth mentioning a new design for ratiometric GECIs based on ddFPs (50). A ddFP consists of a monomer (copy A) that contains a chromophore, and a monomer (copy B) that does not form a chromophore but increases the fluorescence of copy A after AB heterodimer formation. Copy B can form heterodimers with green (GA) or red (RA) copies to form functional green or red ddFPs. The ddFP based GECI is a combination of all three monomer copies that are linked via RA-CaM-B-M13-GA (50). According to the calcium-dependent structural conformation of the CaM and M13 domains the B copy forms either a functional ddFP with the GA or RA copy resulting in calcium-dependent changes in red/green emission ratio changes. The ddFP-based biosensor design opens new possibilities and has been applied to monitor various biological processes (5; 6; 50).

Single-FP GECIs exhibit higher signal-to-noise ratios compared to FRET-based GECIs (151). However, at high magnifications and during prolonged imaging, ratiometric biosensors are preferred as they are internally normalized and can compensate for small focal drifts or variations in GECI concentrations (143). To combine the high signal changes of single-FP GECIs with a ratiometric readout, a reference FP was fused to the C-terminus of single-FP GECOs and GCaMP6f (Waadt et al., In Press) or the reference FP LSSmOrange was inserted within the cpFP of GCaMP6s (Ast et al., In Press, Figure 1).

Choice of the right biosensor variant and design

The huge number of GECIs not only illustrates the variety of biosensor designs but also implies the question why we need so many GECIs and which ones are the best to use for a certain experiment. Efforts to improve GECIs followed the goals to increase the signal-to-noise ratio, modify the binding affinity, improve the binding kinetics, decrease the buffering capacity, make them less invasive, enable subcellular analyses and multicolor approaches (Figure 2). Generally it is recommended to use latest biosensor versions as they likely exhibit improved properties. However, the choice of the right biosensor depends on the available microscopic setup and the experimental requirements (151; 158). Especially for subcellular analyses there are certain biochemical requirements that need to be considered. Analyte concentrations, pH and autofluorescence can vary between different cellular compartments and tissues. To enable reliable and adequate analyses the analyte binding affinity of the biosensor should be close to the steady state analyte concentration in the respective compartment. Most FPs are sensitive to acidic environments (169; 170). Therefore the pKa of a chosen FP should not match the compartment pH, unless monitoring of pH is desired (170). Plants contain many fluorescent compounds (61). Therefore, FPs should be chosen of which excitation and emission can be spectrally separated from the autofluorescent compounds that are present in the imaged compartment.

The different configurations and biosensor designs provide some flexibility for the design of novel direct biosensors. However, it requires an idea about a potential sensory module. If a three-dimensional structure of the sensory module is available, the

biosensor configuration (cpFP- or FRET-based) should be chosen dependent on the structural orientation of the sensory module N- and C-termini. As the further development appears empirical (144), screening technologies using a high combinatorial space of sensory module variants and FRET-pairs (89) eventually leads to the identification of candidate biosensors for further optimization. Optimizations strategies can be structure guided followed by random site directed mutagenesis (4; 185) or guided by large screenings of mutant biosensor libraries in *E. coli* (111; 152; 205). Recently a novel strategy for the identification of cpFP insertion sites into sensory modules has been described (137). In this approach, cpGFP was randomly inserted into maltose-binding protein using a transposon-based cloning strategy followed by FACS sorting and next generation sequencing. Through the use of next generation sequencing the authors could provide a comprehensive view of hotspots for insertion sites (137).

Biological discoveries made with biosensors

Calcium imaging

Calcium is an important signaling molecule that mediates multiple physiological and developmental processes and exhibits rapid fluctuations in concentration in a variety of subcellular compartments (51; 100). Biological findings reported using fluorescent GECIs in plants have been described in currently approximately 80 publications. Here we will focus only on the most important and latest findings generated using fluorescent GECIs.

Calcium imaging in guard cells

Calcium imaging in plants using FRET-based yellow cameleons has been pioneered through work performed in guard cells (9). In guard cells yellow cameleons reported spontaneous cytoplasmic calcium oscillations, but also calcium oscillations that were triggered or modulated via external applications of calcium, ABA, MeJA, H_2O_2, changes in [CO_2], sorbitol, yeast elicitor (YEL), chitosan, allylisothiocyanate, flg22, and chitin (7-9; 82; 90-92; 112; 150; 184; 203; 204). Calcium transients in guard cells can be

artificially imposed via alternate perfusions with hyperpolarizing and depolarizing buffers (7). Using such a system, the optimal calcium pattern for stomatal closure was defined by three 5 min transients at periods of 10 min (7).

A challenge in guard cell calcium signaling research has been the identification of guard cell plasma membrane calcium-permeable (I_{Ca}) channels that are known to be activated by ABA, H_2O_2, MeJA, YEL and Chitosan (70; 92; 134; 150). Studies using yellow cameleons have contributed to the characterization of mutants mediating such calcium responses via I_{Ca} channels. For example, the *gca2* mutant failed to activate I_{Ca} channels in response to H_2O_2 (150) and showed altered calcium patterns in response to external calcium, ABA, and CO_2 (7; 203). Plants with mutations in the calcium-dependent protein kinase *CPK6* were impaired in the generation of ABA-, MeJA- and YEL-induced calcium transients and the activation of I_{Ca} channels (129; 134; 202). *AtrbohD/AtrbohF* double mutants with reduced ROS production were impaired in mediating ABA-induced calcium transients and activation of I_{Ca} channels in guard cells, but responded to H_2O_2 (102). These findings point to the interdependence of calcium-, ABA- and ROS-signaling in guard cells. The interdependence of ABA and JA signaling was highlighted by the findings that the ABA synthesis mutant *aba2-2* was suppressed in MeJA-induced calcium transients but responded to ABA (81). Beyond I_{Ca} channel activity, the use of yellow cameleons also contributed to the characterization of a potential role for vacuolar calcium sequestration (8) and plastidic calcium sensing in guard cell calcium patterns (71; 197).

Guard cell calcium imaging has been mainly performed on epidermal strips that were glued on glass slides (9). Recently, guard cell calcium imaging has been performed on intact leaves using either an inverted microscope to image the abaxial leaf surface while stimulating the adaxial leaf surface, or using an upright microscope for simultaneous imaging and stimulation of the abaxial leaf surface (90). Interestingly, treatments with the pathogen associated molecular patterns flg22 and chitin indicated different calcium response patterns dependent on the imaging setup. Indeed, flg22-induced calcium oscillations in guard cells were only observed at the upright imaging setup (90). In contrast to previous studies that used yellow cameleons, this study

established the red emitting single-FP biosensor R-GECO1 for monitoring cytoplsmic calcium changes in guard cells.

Calcium imaging in pollen tubes and during fertilization

For a broader overview about the role of calcium in pollen tubes please refer to (94; 178). Calcium imaging in pollen tubes was initially established using yellow cameleon YC2.1 in *Lilium longiflorum* and *Nicotiana tabacum* reporting a calcium gradient along with tip focused oscillations (149). During *in vitro* Arabidopsis pollen tube growth, tip focused calcium oscillations were found to be affected by calcium-permeable channel cyclic nucleotide-gated channel CNGC18 (60), ROS-producing NADPH oxidases *AtRBOHH* and *AtRBOHJ* (106), and D-Serine, probably via triggering glutamate receptor-like channels (GLRs) (68; 120). There is also pharmacological and genetic evidence that GLRs play a role in the self-incompatibility response (84).

During *in vivo* pollination in Arabidopsis, cytoplasmic calcium is increased in pollen grains at the pollen tube germination site and oscillates in the pollen tube tip after penetration of the papilla cell wall (86). In papilla cells cytoplasmic calcium increased during pollen hydration at the contact site with the pollen grain, after pollen protrusion, and during pollen tube penetration (86). During double fertilization, synergid cells displayed cytoplasmic calcium oscillations upon contact with the pollen tube tips, which also exhibited calcium oscillations. After growth acceleration, pollen tube burst induced a short calcium transient in the pollen tube tip that spread towards the shank. Pollen tube burst also induced a short calcium transient in eggand central cells as well as rupture of the receptive synergid. Finally another calcium transient appeared after successful fertilization of the egg cell (47; 69; 85; 141). This developmental process has been best illustrated through simultaneous visualization of calcium signals in pollen tubes using R-GECO1 and in synergids using YC3.6 and led to the conclusion that intercellular communications between the pollen tube and synergids coordinate their calcium dynamics and that synergids control sperm delivery through the FERONIA signaling pathway (141).

Calcium imaging in roots

In Arabidopsis roots, calcium imaging using GECIs has been performed to study responses to gravity and mechanical stimulation, cold, changes in extracellular ion compositions (K^+ and Na^+), trivalent ions (Al^{3+}, La^{3+} and Gd^{3+}), osmotic stress, ATP, glutamate, H_2O_2, small peptides pathogen-associated molecular patterns and hormones (18; 27; 42; 74; 90; 98; 112; 126-128; 156)(Waadt et al. In Press). Generally these extracellular treatments induced local and transient cytoplasmic calcium concentration increases. However, the removal of extracellular triggers, such as the osmolyte sorbitol or K^+, through perfusion with control- or depletion-, depolarization- and hyperpolarization buffers also induced calcium transients (18; 98; 112). Interestingly, K^+ deficiency triggered two distinct responses, a rapid and transient calcium increase in the stelar tissue of the elongation zone and a sustained calcium elevation after 18 h in the root hair zone (18). It also has to be noted that commonly used calcium channel blockers such as La^{3+} and Gd^{3+}initially induce rapid calcium transients in roots (156). Therefore, to block calcium channels using these chemicals, prolonged pre-treatments are required.

Gravistimulation triggered calcium signals at the side of the root located towards the gravity vector (128). Gravitropism is tightly associated with auxin signaling (163), and auxin also induced calcium signals in the root elongation zone (128; 172); Waadt et al., In Press). The cyclic nucleotide-gated channel 14 (CNGC14) appeared to be essential for auxin-induced calcium signals and *cngc14* mutants were also impaired in gravitropic responses (172). Several members of the CNGC gene family have been characterized as calcium-permeable channels (60; 196)). Therefore, it is likely that CNGC14 represents the calcium-permeable channel activated by auxin. However, the mechanism for auxin-mediated CNGC14 activation remains to be elucidated.

Local salt stress in the root induced a calcium wave that traveled through the root cortex and endodermis at a speed of ~ 400 µm/s (42). This shoot-ward calcium wave was blocked through pretreatment with calcium channel blockers and affected salt-induced gene expression in the shoot, indicating a long distance systemic salt stress response mediated by calcium (42). The speed of the salt-induced calcium wave was dependent on the vacuolar ion channel TPC1 and the ROS-producing NADPH oxidase

AtRBOHD (42; 54), indicating that an interplay between calcium and ROS is required for long distance calcium signal propagations (40; 178).

Calcium imaging using fluorescent GECIs has not only been applied in Arabidopsis but also in rice and legumes. Compared to Arabidopsis, calcium signals in rice displayed a lower signal amplitude and a greatly increased signal duration in response to glutamate and artificially-imposed calcium signals (19). In legumes GECI-based calcium imaging has been mainly used to study the symbiosis with rhizobial bacteria and mycorrhizal fungi. Rhizobial bacteria and mycorrhizal fungi induced similar calcium patterns and required the same signaling components (95; 145; 173; 174). However, the calcium patterns depended on the stage of infection, with low frequency spiking during intracellular remodeling before infection, and high frequency during the initial stage of apoplastic cell entry (173). Symbiosis-induced calcium changes originated from nuclear membranes in *Medicago truncatula* root hairs and predominantly required the activity of the calcium ATPase MCA8 and cyclic nucleotide-gated channels (30; 34).

Subcellular targeting of GECIs

GECIs have been targeted to several subcellular compartments and membranes (44) with recent targeting of YC3.6 and YC4.6 to the chloroplast stroma (113). While targeting of GECIs into organelles could help to discover organelle specific calcium responses, the attachment of GECIs to the cytoplasmic side of compartment-specific membranes might increase the spatial resolution of calcium response analyses (98).

There are controversial reports on whether the ER functions as a calcium store in plants. GECI-based calcium imaging in the ER lumen in combination with pharmacological treatments that induced calcium depletion from the ER suggested that the pollen tube ER serves as a calcium store (83). On the other hand, imaging in roots indicated that ER calcium followed cytoplasmic calcium patterns in response to several stimuli, however with distinct ER-specific response dynamics (27). Based on these data, it has been suggested that the ER does not function as a source for calcium release for the contribution to cytoplasmic calcium patterns (27).

Similar to the nucleus and ER, calcium signals in peroxysomes, mitochondria and chloroplasts followed cytoplasmic patterns with distinct response kinetics (112; 113). Recently, YC3.6 has been used for the analyses of mitochondrial calcium responses in *micu* mutants that lack a mitochondrial calcium-binding protein with homology to components of the mitochondrial calcium uniporter machinery (195). Mitochondira of *micu* mutants displayed increased basal calcium levels and more rapid calcium responses with higher maximum calcium concentrations in response to ATP and auxin. It has been concluded that MICU functions as a throttle to control mitochondrial calcium uptake (195).

Compared to YC3.6 expressed in the cytoplasm, chloroplast stroma targeted YC3.6 exhibited decreased basal emission ratios in root plastids, indicative for lower basal calcium concentrations there (113). In response to a transition from white to low-intensity blue light, stromal calcium increased steadily, but only in green tissues and independent of extrachloroplastic calcium. Single chloroplasts calcium imaging revealed infrequent stromal calcium spikes, that were dependent on extrachloroplastic calcium (113).

Visualization of reactive oxygen species (ROS) and redox changes

ROS are reactive forms of molecular oxygen and formed as toxic by-products in metabolic reactions but also act as signaling molecules to mediate metabolic-, growth- and developmental processes (93; 199). ROS levels are essential for life and need to be kept above a cytostatic- but below a cytotoxic level to enable proper redox biology (122). ROS levels are regulated through the concerted action of subcellular compartmentalized ROS-producing and ROS-scavenging mechanisms to maintain an optimal cellular redox state (123).

ROS/redox biosensors mainly include intrinsic probes (roGFPs; rxFPs) to monitor the glutathione redox state (2GSH/GSSG-ratio), and extrinsic biosensors for the NAD^+/NADH-ratio, H_2O_2 (HyPer-family and modified roGFPs), and other ROS (26). Early work in plants using ROS/redox biosensors has been summarized previously (41). In plants roGFPs were mainly used to determine the subcellular glutathione redox potential (88; 159; 168), and to measure the glutathione redox state in mutants that are

involved in glutathione biosynthesis (118; 119). Recent experiments using roGFPs were performed to investigate the effects of abiotic stresses on organellar redox dynamics (28). Long term treatments indicated an increased glutathione oxidation in response to several stresses and some degree of organellar specificity dependent on the stress (28; 168).

Short-term analyses of [H_2O_2] changes have been performed in Arabidopsis guard cells and roots using HyPer (20; 43; 77). Analyses indicated that H_2O_2 scavenging in peroxysomes could be stimulated via artificial calcium elevations that might trigger the activation of catalases (43).

pH measurements using pH-sensitive FPs

pH homeostasis is important for secondary transport processes, protein modifications and sorting, and vesicle trafficking (166). Intracellular pH gradients are established through the coordinated activity of H^+-pumps and associated ion transporters and indispensable for cellular compartmentalization and ion homeostasis (17; 166). Work in plants using pH sensitive FPs has been summarized previously (41; 63). Early work was performed using ratiometric pHluorin (Miesenböck et al., 1998 - 9671304) that was optimized for plants (termed phGFP) (130). phGFP enabled the visualization of pH gradients in Arabidopsis roots, with more acidic pH (6.5 - 7) in root-cap cells versus rather alkaline pH (7.3 - 7.6) in the elongation zone and an intermediate pH (7 - 7.3) in the meristematic zone (130). Ratiometric pHluorin reported pH gradients and pH oscillations in tobacco pollen tubes (31). Cytoplasmic pH oscillations were also observed in root hairs using the pH-sensitive GFP (H148D) (125). Ratiometric pHluorin has also been used to estimate apoplastic pH (59), and recently a whole palette of targeted ratiometric pHluorin variants has been used to map the pH in various subcellular compartments and organelles (117; 171).The reported data indicated a pH gradient within the endomembrane system (117; 171).

Compared to phGFP, the pH biosensor Pt-GFP has been successfully established in Arabidopsis to monitor anoxia-induced acidification in roots (165) and to investigate whether changes in [CO_2] affect guard cell pH (200). A third pH biosensor, apo-pHusion, targeted to the apoplast enabled the monitoring of auxin-induced

apoplastic alkalinization in the root elongation zone (62). In hypocotyls apo-pHusion reported auxin- and gravity-induced apoplastic acidifications that were dependent of the canonical TIR/AFB-AUX/IAA auxin signaling pathway (55). pHusion was also used to determine the steady-state pH in the TGN/early endosome and in *trans*-Golgi cisternae (114). Data indicated that reduced V-ATPase activity in the *det3* mutant (167) affected the steady state pH in the TGN/EE but not in *trans*-Golgi cisternae (114). Note that steady state pH values in the TGN/EE (pH 5.6) and *trans*-Golgi (pH 6.3) determined using pHusion (114) were not consistent with values determined using ratiometric pHluorin (TGN pH 6.3 and 6.1, *trans*-Golgi pH 6.9) (117; 171). These differences might result from different calibration protocols. However, due to the more acidic pKa of pHusion, this biosensor more reliably reports the pH in acidic environments (62).

Primary metabolites

Although widely distributed, the concentration of central metabolites can vary across spatial and temporal scales depending on subcellular compartment, cell type, developmental stage, and physiological condition. In many cases, little is known about the concentration of a given metabolite in compartments of plant cells, or how metabolite concentrations are regulated at the cellular or subcellular level. The use of biosensors can help to fill these knowledge gaps, and early studies with metabolite biosensors have proven particularly valuable in both the discovery and characterization of metabolite transport activities. A seminal study which made use of a suite of four glucose biosensors (FLIPglu-Δ13) with a range of affinities ranging from Kd = 170 nM to Kd = 3.2 mM led to a first view that cytosolic glucose concentrations in leaf epidermal cells are lower than root cells (48). FLIPglu-Δ13 glucose biosensors with Kd = 2 μM and 170 nM were responsive to pulsed treatments with exogenous glucose in root cells, but non-responsive in leaf cells owing to apparent saturation prior to treatment (48). The surprisingly large range of biosensors that were responsive to glucose *in vivo* indicated that glucose levels are not under tight homeostatic control in relation to exogenous glucose levels. Subsequently, improvements in root imaging modalities (Figure 3) that coupled tighter temporal control over the liquid perfusion environment resulted in better quantitation of root responses to treatements with exogenous sugars (e.g. glucose and

sucrose (35; 36) and glucose and galactose (67). FLIPglu-Δ13 glucose biosensors that have minimal response to sucrose *in vitro* responded to sucrose perfusion with 60-95% of their response to equimolar glucose treatments when expressed in root cells, demonstrating that sucrolysis is rapid under the conditions tested (36). Long-term perfusion time-course measurements of root growth and the FLII12Pglu-700μ∂6 biosensor that detects glucose and galactose *in vitro* indicated that glucose stabilized root growth in darkness shortly after the start of perfusion but galactose stopped root growth completely after 5 hours of perfusion (67).

Such perfusion experiments can also be used to probe transport properties, for example the accumulation of exogenous glucose as measured using FLIPglu–600μΔ13 and exogenous sucrose as measured using FLIPsuc–90μΔ1 (Figure 4, (36). Results indicated that the sugar transporters known at that time, which depend on the proton gradient, were not responsible for the observed transport properties. A subsequent screen in HEK293T cells expressing Arabidopsis proteins along with a FRET biosensor for glucose led to the discovery of the SWEET family of sugar uniporters that contribute to sugar export *in vivo* (38). A similar progression for studies in amino acid transport involved characterization of partly protonophore insensitive glutamine transport in Arabidopsis roots using a glutamine biosensor (201) followed by the discovery of the UMAMIT amino acid uniporters that can contribute to amino acid export *in vivo* (25; 103; 132). Although the majority of studies have focused on imaging in Arabidopsis, expression of glucose biosensors in rice revealed rapid and reversible glucose increases *in vivo* in response to several signals and stresses beyond glucose, with these responses falling in the detection range of the FLIPglu–2 μΔ13 biosensor with Kd = 2 μM (206).

Recently, an ATP sensor (ATeam (96)) that was originally characterized for use in mammalian cells was deployed in Arabidopsis. ATeam1.03-nD/nA reports $MgATP^{2-}$ and was targeted to the cytosol as well as two ATP producing organelles (i.e. the chloroplast stroma and the mitochondrial matrix) to reveal spatiotemporal patterns of $MgATP^{2-}$ during normal development as well as during energy stress induced by hypoxia (45). In

addition to characterizing $MgATP^{2-}$ steady state patterning, substantial plasticity in $MgATP^{2-}$ was revealed (45).

Hormones

Two FRET-based biosensors for the phytohormone abscisic acid (ABA) have been developed that report on ABA dynamics in response to exogenous ABA or challenge with stress conditions (89; 192). The ABACUS1 (abscisic acid concentration and uptake sensor) was engineered by linking an ABA sensory module (PYL1 fused to a highly truncated ABA interaction domain of ABI1) to edCerulean as FRET donor and edCitrine as FRET acceptor (89). The ABACUS1 biosensor was used to detect reversible and dose-dependent ABA accumulation following pulsed ABA treatments in roots growing in the RootChip16, and it was shown that ABA elimination rate was cell-specific and accelerated by ABA (89). A similar but distinct ABA biosensor, ABAleon2.1, was engineered by fusing an ABA sensory module (PYR1 linked to catalytic domain of the ABI1) to mTurquoise as FRET donor and cpVenus173 as FRET acceptor. ABAleon2.1 reported on endogenous ABA concentrations in response to abiotic stresses and was used to track the long-distance translocation of ABA between root, hypocotyl and shoot tissues in response to exogenous application of ABA (192).

A recent FRET-based biosensor, Gibberellin Perception Sensor 1 (GPS1), detects the phytohormone gibberellin (GA) and was engineered by fusing a GA sensory module (AtGID1C GA receptor linked to the DELLA domain of AtGAI) with edCerulean as FRET donor and edAphrodite as FRET acceptor (Rizza et al. In press). GPS1 responds to nanomolar concentrations of bioactive GAs (e.g. K_d 24 nM for GA_4) and exhibits slow apparent reversibility *in vitro* (Rizza et al. In press). Thus, GPS1 expressed *in vivo* can report increases in GA, but would not report on GA depletions. Expression of GPS1 from a p16 promoter (cite p16 paper), which circumvented silencing observed previously (36; 48; 89), permitted detection of a gradient of GA in dark-grown hypocotyls of wild-type and light signaling mutants (Rizza et al. In press). GPS1 reported higher GA levels in larger cells of the dark-grown hypocotyl as compared with smaller cells near the apical hook and the apparent GA accumulation in the dark was reduced in a phytochrome interacting factor quadruple mutant (Rizza et al. In press). GPS1 also

reported a GA gradient in primary root tips, and this gradient of endogenous GA was mirrored by an accumulation gradient of exogenous GA_4 (Rizza et al. In press). This indicated that GA patterning could be achieved in roots independently of patterns of GA biosynthesis.

Nutrients

Inorganic Phosphate

Plants acquire and assimilate phosphorous in the form of inorganic phosphate (P_i) which is required for important cellular processes such as energy transfer reactions, signal transduction, and enzyme activities. A second-generation FRET-based biosensor that detects inorganic phosphate (P_i), cpFLIPPi, consists of cyanobacterial P_i binding protein fused between eCFP as FRET donor and cpVenus (circularly permuted) as FRET acceptor, was recently developed and used *in planta* (131). The cpFLIPPi biosensor revealed changes in cytosolic P_i concentrations in root epidermal cells in response to P_i starvation and replenishment. In addition, a plastid-targeted version of the cpFLIPPi sensor was used to assess the role of plastidic P_i transporter PHT4;2 in P_i transport (131).

Zinc

High-affinity FRET-based Zn^{2+} sensors, called eCALWY-1, were developed that contain two metal binding domains, ATOX1 and WD4, linked via a flexible linker and flanked by cerulean as FRET donor and citrine as FRET acceptor (190). Binding of Zn^{2+} in between the two metal-binding domains causes a decrease in energy transfer that reports on Zn^{2+} concentrations. Using eCALWY-1 and modified versions in Arabidopsis root cells, Lanquar et. al (104) reported on cytosolic free Zn^{2+} concentrations in roots supplied with varied exogenous Zn^{2+} concentrations using the RootChip (PMID: 22186371). By combining a FRET-based biosensor with the perfusion control afforded by the RootChip, these experiments indicated the involvement of low- and high- affinity uptake systems as well as release of internal stores of Zn^{2+} governing Zn^{2+} homeostasis in living cells (104).

Nitrate and Ammonium Transport

Transporters for ammonium and nitrate ions act as dual function transporter/receptors, or transceptors (10; 97; 109; 191), but the activity status of a specific transporter is difficult to assess within a living plant. De Michelle et al. (46) created an transport-activity biosensor by inserting a circularly permutated GFP (mcpGFP) into the cytosolic loop of the Arabidopsis ammonium transporter AMT1;3. This intensiometric approach is based on tracking mcpGFP fluorescence changes that result from conformational changes in AMT1;3 that occur during transport. Yeast cells expressing AMT1;3-mcpGFP biosensors (AmTracs) showed concentration-dependent fluorescence intensity changes in response to ammonium chloride treatments that correlated with the transport activity of AMT1;3. Two more ammonium transport activity state biosensors were created by utilizing the same approach, and these chimeric AmTrac1;2 and MepTrac biosensors maintained the transporter activity in yeast cells and exhibited intensiometric fluorescence responses to ammonium treatments (46). Ast et al. (12) characterized the photophysical properties of different AmTrac biosensors and replaced key amino acid residues in the mcpGFP of AmTrac to construct a set of ratiometric dual-emission AmTrac biosensors named deAmTracs (12).

Ho and Frommer (78) sandwiched the nitrate transceptor CHL1 between mCerulean and Aphrodite, and exploited conformational rearrangements during the transporter cycle that quenched fluorescence of the mCerulean moiety. This chimera, NiTrac1, was used to report on the movement of nitrate through yeast cell membranes. Measurements of the NiTrac1 response in yeast cells demonstrated nitrate-induced quenching that was reversible in nature after removal of nitrate (78). Furthermore, similar constructs for the oligopeptide transporters PTR1, 2, 4, and 5 from Arabidopsis were created and found to exhibit peptide-specific quenching. Furthermore, NiTrac1 expressed in yeast was used to facilitate testing the effects of CHL1 mutations and protein-protein interactions (78).

Taken together, these investigations utilizing the activity state sensors in yeast cells have significantly increased our understanding of transporter behavior, though application of these biosensors to *in planta* characterizations awaits further experimentation.

Multicolor and Multiparameter Analyses Using Fluorescent Reporters

Multicolor and multiparameter analyses rely on the principle that two or more genetically encoded fluorescent biosensors are co-expressed in the same plant and tissue and imaged simultaneously at the microscope. Multicolor fluorescent biosensors were first developed for calcium (3; 205) summarized in (151), and are also available for ROS/redox- (26) and pH measurements (21). Most fluorescent biosensors are FRET-based or green-emitting (https://codex.dpb.carnegiescience.edu/db/biosensor). Therefore, key for the achievement of multicolor/multiparameter analyses was the development of red-emitting fluorescent biosensors.

Multicolor analyses describe the simultaneous imaging of the same analyte using fluorescent biosensors of separable emissions. Such approaches enable analyses with increased spatial resolution if the analyte is imaged from distinct subcellular locations or cell types. Multicolor calcium imaging has been described in which the cytoplasmic and nuclear localized red-emitting R-GECO1 was co-expressed with the cytoplasmic FRET-based YC3.6 (90). Although, this study mainly compared the *in vivo* properties of both GECIs, it demonstrated that R-GECO1 exhibited more than 10-fold increased signal changes compared to YC3.6 in response to ATP and hyperpolarization buffer (90). Through the expression of R-GECO1 in pollen tubes and YC3.6 in synergids it was for the first time possible to spatially resolve calcium signals during double fertilization in both cell types simultaneously (141), demonstrating the huge potential of multicolor imaging approaches in plants.

Multiparameter analyses combine fluorescent reporters for distinct analytes. This has been recently employed to simultaneously image ABA using the FRET-based biosensor ABAleon2.1 and calcium using R-GECO1 (192; 205) Waadt et al., In Press). Hormone response analyses in young roots indicated that although ABA was rapidly taken up, it did not trigger rapid calcium signals. On the other hand, auxin induced calcium signals, but did not trigger rapid ABA concentration changes (Waadt et al., In Press). Through the use of R-GECO1 and other red-emitting biosensors for calcium, ROS/redox or pH (see above) it is now possible to resolve and correlate the dynamic changes of at least two of these molecules at the same time. In addition, red-emitting biosensors have the potential to be combined with any FRET-based and blue- or green-

emitting biosensors. Finally, it is also possible to combine direct FRET-based readouts with indirect red-emitting transcriptional readouts.

Summary and Outlook

Molecules or molecular events whose variation in concentration or activity is physiologically relevant are prime targets for biosensing approaches. In the context of multiorganellar and multicellular eukaryotes, the spatiotemporal information obtainable using biosensors is particularly important. This is true for understanding both the regulatory and biochemical activities that influence the spatiotemporal patterns of a molecule or molecular event of interest and for the physiological consequences of such patterns. Starting from initial biosensor engineering, *in vivo* analysis of several analytes has now progressed sufficiently through optimization of biosensor performance, expression *in planta*, and imaging modalities such that novel spatiotemporal patterns are being discovered and characterized in a variety of biological systems. Most analytes still lack biosensors, however, and most extant biosensors have yet to be deployed in plants, and thus the potential of biosensor-based analysis is only just beginning to be tapped. Fortunately, new biosensors continue to be engineered based on high-specificity sensory proteins, e.g. for MAP Kinase signaling (P. Krysan, personal communications), and there is further promise for a more generalized approach based on incorporating RNA aptamers or antibodies selected to have the requisite specificity into genetically encoded biosensors (142). Furthermore, direct biosensors developed for use in other organisms are often functional in plants with little to no reengineering (45; 104), and thus the barrier to the first application of an extant biosensor in plants is often low.

Acknowledgements

A.W. and A.M.J. were supported by a Gatsby Research Fellowship awarded to A.M.J. R.W. was supported by the Deutsche Forschungsgemeinschaft (WA 3768/1-1).

Figure Legends

Figure 1. Twenty years of fluorescent GECIs. Evolution of genetically-encoded calcium indicators over the last 20 years with biosensors plotted as dots on the year of publication that are colored according to the emission wavelength of their constituent fluorophores. Single FP biosensors are plotted at left and double-FP biosensors at right.

Figure 2. Biosensor considerations. The successful engineering and use of genetically encoded biosensors relies on appropriate consideration of the key parameters diagrammed. To offer an example, the contrasting features and limitations of current ABA biosensors [ABACUS1-2μ and ABAleon2.1 (89; 192)] as well as a idealized ABA biosensors are plotted. An idealised biosensor should display high dynamic range of biosensor response, a dynamic range of analyte detection that is physiologically relevant, as well as high orthogonality.

Figure 3. Biosensor imaging modalities. Schematic illustrations to show various imaging modalities for plants expressing biosensors (*Currently presented as photos, suggest to convert to schematics/diagrams with the assistance of ARPB artists*). (*a*) Agar- or vacuum grease-based approaches to monitor biosensor responses to short-term experimental treatments (128; 192), (Rizza et al, *in press*), (*b*) Chambers using adhesive restraint to monitor biosensor response to short-term treatments (35), (*c*) Perfusion based chambers using mechanical restraint to monitor biosensor responses (long-term or short-term) to various treatments using custom-built chambers (99; 164), IBIDI slides (37), and SecureSeal^{TM} (157), (*d*) Microfluidics-based perfusion chambers to monitor biosensor responses (long-term or short-term) in plant roots (67; 177).

Figure 4. Biosensors for studying transport. (Left) Genetically encoded biosensors have been used *in planta* to monitor accumulation and elimination rates of during and following pulsed application of exogenous analytes (e.g. (48)). This approach allows the interrogation of transport activities *in vivo* and can be applied to indirectly probe affinity (e.g. (89)), mechanisms (e.g. (36)), and spatiotemporal patterning (e.g. Rizza et al. In press) of transport activities. Also, such analyses can reveal quantitative molecular phenotypes in mutant lines expressing biosensors (e.g. (131)). (Right) Biosensors have also been used in heterologous systems to screen for novel plant transporters (e.g. SWEET1 (38)), and, through the use of sensorized transporters, to rapidly interrogate the effects of mutations and protein interactions on activity of plant transporters (e.g. NRT1.1/CHL1/NPF6.3 (78)).

References

1. Achard P, Cheng H, De Grauwe L, Decat J, Schoutteten H, et al. 2006. Integration of plant responses to environmentally activated phytohormonal signals. *Science* 311:91-4
2. Achard P, Liao L, Jiang C, Desnos T, Bartlett J, et al. 2007. DELLAs contribute to plant photomorphogenesis. *Plant Physiol* 143:1163-72
3. Akerboom J, Carreras Calderon N, Tian L, Wabnig S, Prigge M, et al. 2013. Genetically encoded calcium indicators for multi-color neural activity imaging and combination with optogenetics. *Front Mol Neurosci* 6:2
4. Akerboom J, Chen TW, Wardill TJ, Tian L, Marvin JS, et al. 2012. Optimization of a GCaMP calcium indicator for neural activity imaging. *J Neurosci* 32:13819-40
5. Alford SC, Abdelfattah AS, Ding Y, Campbell RE. 2012. A fluorogenic red fluorescent protein heterodimer. *Chem Biol* 19:353-60
6. Alford SC, Wu J, Zhao Y, Campbell RE, Knopfel T. 2013. Optogenetic reporters. *Biol Cell* 105:14-29
7. Allen GJ, Chu SP, Harrington CL, Schumacher K, Hoffmann T, et al. 2001. A defined range of guard cell calcium oscillation parameters encodes stomatal movements. *Nature* 411:1053-7
8. Allen GJ, Chu SP, Schumacher K, Shimazaki CT, Vafeados D, et al. 2000. Alteration of stimulus-specific guard cell calcium oscillations and stomatal closing in Arabidopsis det3 mutant. *Science* 289:2338-42
9. Allen GJ, Kwak JM, Chu SP, Llopis J, Tsien RY, et al. 1999. Cameleon calcium indicator reports cytoplasmic calcium dynamics in Arabidopsis guard cells. *Plant J* 19:735-47
10. Andrade SL, Einsle O. 2007. The Amt/Mep/Rh family of ammonium transport proteins. *Mol Membr Biol* 24:357-65
11. Arosio D, Ricci F, Marchetti L, Gualdani R, Albertazzi L, Beltram F. 2010. Simultaneous intracellular chloride and pH measurements using a GFP-based sensor. *Nat Methods* 7:516-8
12. Ast C, De Michele R, Kumke MU, Frommer WB. 2015. Single-fluorophore membrane transport activity sensors with dual-emission read-out. *Elife* 4:e07113
13. Baird GS, Zacharias DA, Tsien RY. 1999. Circular permutation and receptor insertion within green fluorescent proteins. *Proc Natl Acad Sci U S A* 96:11241-6
14. Band LR, Wells DM, Fozard JA, Ghetiu T, French AP, et al. 2014. Systems analysis of auxin transport in the Arabidopsis root apex. *Plant Cell* 26:862-75
15. Band LR, Wells DM, Larrieu A, Sun J, Middleton AM, et al. 2012. Root gravitropism is regulated by a transient lateral auxin gradient controlled by a tipping-point mechanism. *Proc Natl Acad Sci U S A* 109:4668-73
16. Barbez E, Dunser K, Gaidora A, Lendl T, Busch W. 2017. Auxin steers root cell expansion via apoplastic pH regulation in Arabidopsis thaliana. *Proc Natl Acad Sci U S A* 114:E4884-E93
17. Bassil E, Blumwald E. 2014. The ins and outs of intracellular ion homeostasis: NHX-type cation/H(+) transporters. *Curr Opin Plant Biol* 22:1-6
18. Behera S, Long Y, Schmitz-Thom I, Wang XP, Zhang C, et al. 2017. Two spatially and temporally distinct Ca2+ signals convey Arabidopsis thaliana responses to K+ deficiency. *New Phytol* 213:739-50
19. Behera S, Wang N, Zhang C, Schmitz-Thom I, Strohkamp S, et al. 2015. Analyses of Ca2+ dynamics using a ubiquitin-10 promoter-driven Yellow Cameleon 3.6 indicator reveal reliable transgene expression and differences in cytoplasmic Ca2+ responses in Arabidopsis and rice (Oryza sativa) roots. *New Phytol* 206:751-60

20. Belousov VV, Fradkov AF, Lukyanov KA, Staroverov DB, Shakhbazov KS, et al. 2006. Genetically encoded fluorescent indicator for intracellular hydrogen peroxide. *Nat Methods* 3:281-6
21. Bencina M. 2013. Illumination of the spatial order of intracellular pH by genetically encoded pH-sensitive sensors. *Sensors (Basel)* 13:16736-58
22. Bencivenga S, Simonini S, Benkova E, Colombo L. 2012. The transcription factors BEL1 and SPL are required for cytokinin and auxin signaling during ovule development in Arabidopsis. *Plant Cell* 24:2886-97
23. Benkova E, Michniewicz M, Sauer M, Teichmann T, Seifertova D, et al. 2003. Local, efflux-dependent auxin gradients as a common module for plant organ formation. *Cell* 115:591-602
24. Berlin S, Carroll EC, Newman ZL, Okada HO, Quinn CM, et al. 2015. Photoactivatable genetically encoded calcium indicators for targeted neuronal imaging. *Nat Methods* 12:852-8
25. Besnard J, Pratelli R, Zhao C, Sonawala U, Collakova E, et al. 2016. UMAMIT14 is an amino acid exporter involved in phloem unloading in Arabidopsis roots. *J Exp Bot* 67:6385-97
26. Bilan DS, Belousov VV. 2017. New tools for redox biology: From imaging to manipulation. *Free Radic Biol Med* 109:167-88
27. Bonza MC, Loro G, Behera S, Wong A, Kudla J, Costa A. 2013. Analyses of Ca2+ accumulation and dynamics in the endoplasmic reticulum of Arabidopsis root cells using a genetically encoded Cameleon sensor. *Plant Physiol* 163:1230-41
28. Bratt A, Rosenwasser S, Meyer A, Fluhr R. 2016. Organelle redox autonomy during environmental stress. *Plant Cell Environ* 39:1909-19
29. Brunoud G, Wells DM, Oliva M, Larrieu A, Mirabet V, et al. 2012. A novel sensor to map auxin response and distribution at high spatio-temporal resolution. *Nature* 482:103-6
30. Capoen W, Sun J, Wysham D, Otegui MS, Venkateshwaran M, et al. 2011. Nuclear membranes control symbiotic calcium signaling of legumes. *Proc Natl Acad Sci U S A* 108:14348-53
31. Certal AC, Almeida RB, Carvalho LM, Wong E, Moreno N, et al. 2008. Exclusion of a proton ATPase from the apical membrane is associated with cell polarity and tip growth in Nicotiana tabacum pollen tubes. *Plant Cell* 20:614-34
32. Chaiwanon J, Wang ZY. 2015. Spatiotemporal brassinosteroid signaling and antagonism with auxin pattern stem cell dynamics in Arabidopsis roots. *Curr Biol* 25:1031-42
33. Chapleau RR, Blomberg R, Ford PC, Sagermann M. 2008. Design of a highly specific and noninvasive biosensor suitable for real-time in vivo imaging of mercury (II) uptake. *Protein Sci* 17:614-22
34. Charpentier M, Sun J, Vaz Martins T, Radhakrishnan GV, Findlay K, et al. 2016. Nuclear-localized cyclic nucleotide-gated channels mediate symbiotic calcium oscillations. *Science* 352:1102-5
35. Chaudhuri B, Hormann F, Frommer WB. 2011. Dynamic imaging of glucose flux impedance using FRET sensors in wild-type Arabidopsis plants. *J Exp Bot* 62:2411-7
36. Chaudhuri B, Hormann F, Lalonde S, Brady SM, Orlando DA, et al. 2008. Protonophore- and pH-insensitive glucose and sucrose accumulation detected by FRET nanosensors in Arabidopsis root tips. *Plant J* 56:948-62
37. Chebli Y, Pujol L, Shojaeifard A, Brouwer I, van Loon JJ, Geitmann A. 2013. Cell wall assembly and intracellular trafficking in plant cells are directly affected by changes in the magnitude of gravitational acceleration. *PLoS One* 8:e58246
38. Chen LQ, Hou BH, Lalonde S, Takanaga H, Hartung ML, et al. 2010. Sugar transporters for intercellular exchange and nutrition of pathogens. *Nature* 468:527-32
39. Chen TW, Wardill TJ, Sun Y, Pulver SR, Renninger SL, et al. 2013. Ultrasensitive fluorescent proteins for imaging neuronal activity. *Nature* 499:295-300
40. Choi WG, Hilleary R, Swanson SJ, Kim SH, Gilroy S. 2016. Rapid, Long-Distance Electrical and Calcium Signaling in Plants. *Annu Rev Plant Biol* 67:287-307

41. Choi WG, Swanson SJ, Gilroy S. 2012. High-resolution imaging of Ca2+ , redox status, ROS and pH using GFP biosensors. *Plant J* 70:118-28
42. Choi WG, Toyota M, Kim SH, Hilleary R, Gilroy S. 2014. Salt stress-induced Ca2+ waves are associated with rapid, long-distance root-to-shoot signaling in plants. *Proc Natl Acad Sci U S A* 111:6497-502
43. Costa A, Drago I, Behera S, Zottini M, Pizzo P, et al. 2010. H2O2 in plant peroxisomes: an in vivo analysis uncovers a Ca(2+)-dependent scavenging system. *Plant J* 62:760-72
44. Costa A, Kudla J. 2015. Colorful insights: advances in imaging drive novel breakthroughs in Ca2+ signaling. *Mol Plant* 8:352-5
45. De Col V, Fuchs P, Nietzel T, Elsasser M, Voon CP, et al. 2017. ATP sensing in living plant cells reveals tissue gradients and stress dynamics of energy physiology. *Elife* 6
46. De Michele R, Ast C, Loque D, Ho CH, Andrade S, et al. 2013. Fluorescent sensors reporting the activity of ammonium transceptors in live cells. *Elife* 2:e00800
47. Denninger P, Bleckmann A, Lausser A, Vogler F, Ott T, et al. 2014. Male-female communication triggers calcium signatures during fertilization in Arabidopsis. *Nat Commun* 5:4645
48. Deuschle K, Chaudhuri B, Okumoto S, Lager I, Lalonde S, Frommer WB. 2006. Rapid metabolism of glucose detected with FRET glucose nanosensors in epidermal cells and intact roots of Arabidopsis RNA-silencing mutants. *Plant Cell* 18:2314-25
49. Dill A, Jung HS, Sun TP. 2001. The DELLA motif is essential for gibberellin-induced degradation of RGA. *Proc Natl Acad Sci U S A* 98:14162-7
50. Ding Y, Li J, Enterina JR, Shen Y, Zhang I, et al. 2015. Ratiometric biosensors based on dimerization-dependent fluorescent protein exchange. *Nat Methods* 12:195-8
51. Dodd AN, Kudla J, Sanders D. 2010. The language of calcium signaling. *Annu Rev Plant Biol* 61:593-620
52. Dohmann EM, Nill C, Schwechheimer C. 2010. DELLA proteins restrain germination and elongation growth in Arabidopsis thaliana COP9 signalosome mutants. *Eur J Cell Biol* 89:163-8
53. Duan L, Dietrich D, Ng CH, Chan PM, Bhalerao R, et al. 2013. Endodermal ABA signaling promotes lateral root quiescence during salt stress in Arabidopsis seedlings. *Plant Cell* 25:324-41
54. Evans MJ, Choi WG, Gilroy S, Morris RJ. 2016. A ROS-Assisted Calcium Wave Dependent on the AtRBOHD NADPH Oxidase and TPC1 Cation Channel Propagates the Systemic Response to Salt Stress. *Plant Physiol* 171:1771-84
55. Fendrych M, Leung J, Friml J. 2016. TIR1/AFB-Aux/IAA auxin perception mediates rapid cell wall acidification and growth of Arabidopsis hypocotyls. *Elife* 5
56. Figueiredo DD, Batista RA, Roszak PJ, Hennig L, Kohler C. 2016. Auxin production in the endosperm drives seed coat development in Arabidopsis. *Elife* 5
57. Fosque BF, Sun Y, Dana H, Yang CT, Ohyama T, et al. 2015. Neural circuits. Labeling of active neural circuits in vivo with designed calcium integrators. *Science* 347:755-60
58. Galietta LJ, Haggie PM, Verkman AS. 2001. Green fluorescent protein-based halide indicators with improved chloride and iodide affinities. *FEBS Lett* 499:220-4
59. Gao D, Knight MR, Trewavas AJ, Sattelmacher B, Plieth C. 2004. Self-reporting Arabidopsis expressing pH and [Ca2+] indicators unveil ion dynamics in the cytoplasm and in the apoplast under abiotic stress. *Plant Physiol* 134:898-908
60. Gao QF, Gu LL, Wang HQ, Fei CF, Fang X, et al. 2016. Cyclic nucleotide-gated channel 18 is an essential Ca2+ channel in pollen tube tips for pollen tube guidance to ovules in Arabidopsis. *Proc Natl Acad Sci U S A* 113:3096-101
61. Garcia-Plazaola JI, Fernandez-Marin B, Duke SO, Hernandez A, Lopez-Arbeloa F, Becerril JM. 2015. Autofluorescence: Biological functions and technical applications. *Plant Sci* 236:136-45

62. Gjetting KS, Ytting CK, Schulz A, Fuglsang AT. 2012. Live imaging of intra- and extracellular pH in plants using pHusion, a novel genetically encoded biosensor. *J Exp Bot* 63:3207-18
63. Gjetting SK, Schulz A, Fuglsang AT. 2013. Perspectives for using genetically encoded fluorescent biosensors in plants. *Front Plant Sci* 4:234
64. Gordon SP, Chickarmane VS, Ohno C, Meyerowitz EM. 2009. Multiple feedback loops through cytokinin signaling control stem cell number within the Arabidopsis shoot meristem. *Proc Natl Acad Sci U S A* 106:16529-34
65. Gould SJ, Subramani S. 1988. Firefly luciferase as a tool in molecular and cell biology. *Anal Biochem* 175:5-13
66. Griesbeck O, Baird GS, Campbell RE, Zacharias DA, Tsien RY. 2001. Reducing the environmental sensitivity of yellow fluorescent protein. Mechanism and applications. *J Biol Chem* 276:29188-94
67. Grossmann G, Guo WJ, Ehrhardt DW, Frommer WB, Sit RV, et al. 2011. The RootChip: an integrated microfluidic chip for plant science. *Plant Cell* 23:4234-40
68. Gutermuth T, Lassig R, Portes MT, Maierhofer T, Romeis T, et al. 2013. Pollen tube growth regulation by free anions depends on the interaction between the anion channel SLAH3 and calcium-dependent protein kinases CPK2 and CPK20. *Plant Cell* 25:4525-43
69. Hamamura Y, Nishimaki M, Takeuchi H, Geitmann A, Kurihara D, Higashiyama T. 2014. Live imaging of calcium spikes during double fertilization in Arabidopsis. *Nat Commun* 5:4722
70. Hamilton DW, Hills A, Kohler B, Blatt MR. 2000. Ca2+ channels at the plasma membrane of stomatal guard cells are activated by hyperpolarization and abscisic acid. *Proc Natl Acad Sci U S A* 97:4967-72
71. Han S, Tang R, Anderson LK, Woerner TE, Pei ZM. 2003. A cell surface receptor mediates extracellular Ca(2+) sensing in guard cells. *Nature* 425:196-200
72. Hanson GT, Aggeler R, Oglesbee D, Cannon M, Capaldi RA, et al. 2004. Investigating mitochondrial redox potential with redox-sensitive green fluorescent protein indicators. *J Biol Chem* 279:13044-53
73. Hanson GT, McAnaney TB, Park ES, Rendell ME, Yarbrough DK, et al. 2002. Green fluorescent protein variants as ratiometric dual emission pH sensors. 1. Structural characterization and preliminary application. *Biochemistry* 41:15477-88
74. Haruta M, Monshausen G, Gilroy S, Sussman MR. 2008. A cytoplasmic Ca2+ functional assay for identifying and purifying endogenous cell signaling peptides in Arabidopsis seedlings: identification of AtRALF1 peptide. *Biochemistry* 47:6311-21
75. Heim N, Griesbeck O. 2004. Genetically encoded indicators of cellular calcium dynamics based on troponin C and green fluorescent protein. *J Biol Chem* 279:14280-6
76. Heisler MG, Ohno C, Das P, Sieber P, Reddy GV, et al. 2005. Patterns of auxin transport and gene expression during primordium development revealed by live imaging of the Arabidopsis inflorescence meristem. *Curr Biol* 15:1899-911
77. Hernandez-Barrera A, Velarde-Buendia A, Zepeda I, Sanchez F, Quinto C, et al. 2015. Hyper, a hydrogen peroxide sensor, indicates the sensitivity of the Arabidopsis root elongation zone to aluminum treatment. *Sensors (Basel)* 15:855-67
78. Ho CH, Frommer WB. 2014. Fluorescent sensors for activity and regulation of the nitrate transceptor CHL1/NRT1.1 and oligopeptide transporters. *Elife* 3:e01917
79. Hoi H, Matsuda T, Nagai T, Campbell RE. 2013. Highlightable Ca2+ indicators for live cell imaging. *J Am Chem Soc* 135:46-9
80. Horikawa K, Yamada Y, Matsuda T, Kobayashi K, Hashimoto M, et al. 2010. Spontaneous network activity visualized by ultrasensitive Ca(2+) indicators, yellow Cameleon-Nano. *Nat Methods* 7:729-32

81. Hossain MA, Munemasa S, Uraji M, Nakamura Y, Mori IC, Murata Y. 2011. Involvement of endogenous abscisic acid in methyl jasmonate-induced stomatal closure in Arabidopsis. *Plant Physiol* 156:430-8
82. Islam MM, Hossain MA, Jannat R, Munemasa S, Nakamura Y, et al. 2010. Cytosolic alkalization and cytosolic calcium oscillation in Arabidopsis guard cells response to ABA and MeJA. *Plant Cell Physiol* 51:1721-30
83. Iwano M, Entani T, Shiba H, Kakita M, Nagai T, et al. 2009. Fine-tuning of the cytoplasmic Ca2+ concentration is essential for pollen tube growth. *Plant Physiol* 150:1322-34
84. Iwano M, Ito K, Fujii S, Kakita M, Asano-Shimosato H, et al. 2015. Calcium signalling mediates self-incompatibility response in the Brassicaceae. *Nat Plants* 1:15128
85. Iwano M, Ngo QA, Entani T, Shiba H, Nagai T, et al. 2012. Cytoplasmic Ca2+ changes dynamically during the interaction of the pollen tube with synergid cells. *Development* 139:4202-9
86. Iwano M, Shiba H, Miwa T, Che FS, Takayama S, et al. 2004. Ca2+ dynamics in a pollen grain and papilla cell during pollination of Arabidopsis. *Plant Physiol* 136:3562-71
87. Jayaraman S, Haggie P, Wachter RM, Remington SJ, Verkman AS. 2000. Mechanism and cellular applications of a green fluorescent protein-based halide sensor. *J Biol Chem* 275:6047-50
88. Jiang K, Schwarzer C, Lally E, Zhang S, Ruzin S, et al. 2006. Expression and characterization of a redox-sensing green fluorescent protein (reduction-oxidation-sensitive green fluorescent protein) in Arabidopsis. *Plant Physiol* 141:397-403
89. Jones AM, Danielson JA, Manojkumar SN, Lanquar V, Grossmann G, Frommer WB. 2014. Abscisic acid dynamics in roots detected with genetically encoded FRET sensors. *Elife* 3:e01741
90. Keinath NF, Waadt R, Brugman R, Schroeder JI, Grossmann G, et al. 2015. Live Cell Imaging with R-GECO1 Sheds Light on flg22- and Chitin-Induced Transient [Ca(2+)]cyt Patterns in Arabidopsis. *Mol Plant* 8:1188-200
91. Khokon MA, Jahan MS, Rahman T, Hossain MA, Muroyama D, et al. 2011. Allyl isothiocyanate (AITC) induces stomatal closure in Arabidopsis. *Plant Cell Environ* 34:1900-6
92. Klusener B, Young JJ, Murata Y, Allen GJ, Mori IC, et al. 2002. Convergence of calcium signaling pathways of pathogenic elicitors and abscisic acid in Arabidopsis guard cells. *Plant Physiol* 130:2152-63
93. Kocsy G, Tari I, Vankova R, Zechmann B, Gulyas Z, et al. 2013. Redox control of plant growth and development. *Plant Sci* 211:77-91
94. Konrad KR, Wudick MM, Feijo JA. 2011. Calcium regulation of tip growth: new genes for old mechanisms. *Curr Opin Plant Biol* 14:721-30
95. Kosuta S, Hazledine S, Sun J, Miwa H, Morris RJ, et al. 2008. Differential and chaotic calcium signatures in the symbiosis signaling pathway of legumes. *Proc Natl Acad Sci U S A* 105:9823-8
96. Kotera I, Iwasaki T, Imamura H, Noji H, Nagai T. 2010. Reversible dimerization of Aequorea victoria fluorescent proteins increases the dynamic range of FRET-based indicators. *ACS Chem Biol* 5:215-22
97. Kotur Z, Mackenzie N, Ramesh S, Tyerman SD, Kaiser BN, Glass AD. 2012. Nitrate transport capacity of the Arabidopsis thaliana NRT2 family members and their interactions with AtNAR2.1. *New Phytol* 194:724-31
98. Krebs M, Held K, Binder A, Hashimoto K, Den Herder G, et al. 2012. FRET-based genetically encoded sensors allow high-resolution live cell imaging of Ca(2)(+) dynamics. *Plant J* 69:181-92
99. Krebs M, Schumacher K. 2013. Live cell imaging of cytoplasmic and nuclear Ca2+ dynamics in Arabidopsis roots. *Cold Spring Harb Protoc* 2013:776-80
100. Kudla J, Batistic O, Hashimoto K. 2010. Calcium signals: the lead currency of plant information processing. *Plant Cell* 22:541-63

101. Kuner T, Augustine GJ. 2000. A genetically encoded ratiometric indicator for chloride: capturing chloride transients in cultured hippocampal neurons. *Neuron* 27:447-59
102. Kwak JM, Mori IC, Pei ZM, Leonhardt N, Torres MA, et al. 2003. NADPH oxidase AtrbohD and AtrbohF genes function in ROS-dependent ABA signaling in Arabidopsis. *EMBO J* 22:2623-33
103. Ladwig F, Stahl M, Ludewig U, Hirner AA, Hammes UZ, et al. 2012. Siliques are Red1 from Arabidopsis acts as a bidirectional amino acid transporter that is crucial for the amino acid homeostasis of siliques. *Plant Physiol* 158:1643-55
104. Lanquar V, Grossmann G, Vinkenborg JL, Merkx M, Thomine S, Frommer WB. 2014. Dynamic imaging of cytosolic zinc in Arabidopsis roots combining FRET sensors and RootChip technology. *New Phytol* 202:198-208
105. Larrieu A, Champion A, Legrand J, Lavenus J, Mast D, et al. 2015. A fluorescent hormone biosensor reveals the dynamics of jasmonate signalling in plants. *Nat Commun* 6:6043
106. Lassig R, Gutermuth T, Bey TD, Konrad KR, Romeis T. 2014. Pollen tube NAD(P)H oxidases act as a speed control to dampen growth rate oscillations during polarized cell growth. *Plant J* 78:94-106
107. Le J, Liu XG, Yang KZ, Chen XL, Zou JJ, et al. 2014. Auxin transport and activity regulate stomatal patterning and development. *Nat Commun* 5:3090
108. Lemke EA, Schultz C. 2011. Principles for designing fluorescent sensors and reporters. *Nat Chem Biol* 7:480-3
109. Leran S, Varala K, Boyer JC, Chiurazzi M, Crawford N, et al. 2014. A unified nomenclature of NITRATE TRANSPORTER 1/PEPTIDE TRANSPORTER family members in plants. *Trends Plant Sci* 19:5-9
110. Liao CY, Smet W, Brunoud G, Yoshida S, Vernoux T, Weijers D. 2015. Reporters for sensitive and quantitative measurement of auxin response. *Nat Methods* 12:207-10, 2 p following 10
111. Litzlbauer J, Schifferer M, Ng D, Fabritius A, Thestrup T, Griesbeck O. 2015. Large Scale Bacterial Colony Screening of Diversified FRET Biosensors. *PLoS One* 10:e0119860
112. Loro G, Drago I, Pozzan T, Schiavo FL, Zottini M, Costa A. 2012. Targeting of Cameleons to various subcellular compartments reveals a strict cytoplasmic/mitochondrial Ca(2)(+) handling relationship in plant cells. *Plant J* 71:1-13
113. Loro G, Wagner S, Doccula FG, Behera S, Weinl S, et al. 2016. Chloroplast-Specific in Vivo Ca2+ Imaging Using Yellow Cameleon Fluorescent Protein Sensors Reveals Organelle-Autonomous Ca2+ Signatures in the Stroma. *Plant Physiol* 171:2317-30
114. Luo Y, Scholl S, Doering A, Zhang Y, Irani NG, et al. 2015. V-ATPase activity in the TGN/EE is required for exocytosis and recycling in Arabidopsis. *Nat Plants* 1:15094
115. Mank M, Santos AF, Direnberger S, Mrsic-Flogel TD, Hofer SB, et al. 2008. A genetically encoded calcium indicator for chronic in vivo two-photon imaging. *Nat Methods* 5:805-11
116. Marchive C, Roudier F, Castaings L, Brehaut V, Blondet E, et al. 2013. Nuclear retention of the transcription factor NLP7 orchestrates the early response to nitrate in plants. *Nat Commun* 4:1713
117. Martiniere A, Bassil E, Jublanc E, Alcon C, Reguera M, et al. 2013. In vivo intracellular pH measurements in tobacco and Arabidopsis reveal an unexpected pH gradient in the endomembrane system. *Plant Cell* 25:4028-43
118. Marty L, Siala W, Schwarzlander M, Fricker MD, Wirtz M, et al. 2009. The NADPH-dependent thioredoxin system constitutes a functional backup for cytosolic glutathione reductase in Arabidopsis. *Proc Natl Acad Sci U S A* 106:9109-14
119. Meyer AJ, Brach T, Marty L, Kreye S, Rouhier N, et al. 2007. Redox-sensitive GFP in Arabidopsis thaliana is a quantitative biosensor for the redox potential of the cellular glutathione redox buffer. *Plant J* 52:973-86

120. Michard E, Lima PT, Borges F, Silva AC, Portes MT, et al. 2011. Glutamate receptor-like genes form Ca2+ channels in pollen tubes and are regulated by pistil D-serine. *Science* 332:434-7
121. Miesenbock G, De Angelis DA, Rothman JE. 1998. Visualizing secretion and synaptic transmission with pH-sensitive green fluorescent proteins. *Nature* 394:192-5
122. Mittler R. 2017. ROS Are Good. *Trends Plant Sci* 22:11-9
123. Mittler R, Vanderauwera S, Gollery M, Van Breusegem F. 2004. Reactive oxygen gene network of plants. *Trends Plant Sci* 9:490-8
124. Miyawaki A, Llopis J, Heim R, McCaffery JM, Adams JA, et al. 1997. Fluorescent indicators for Ca2+ based on green fluorescent proteins and calmodulin. *Nature* 388:882-7
125. Monshausen GB, Bibikova TN, Messerli MA, Shi C, Gilroy S. 2007. Oscillations in extracellular pH and reactive oxygen species modulate tip growth of Arabidopsis root hairs. *Proc Natl Acad Sci U S A* 104:20996-1001
126. Monshausen GB, Bibikova TN, Weisenseel MH, Gilroy S. 2009. Ca2+ regulates reactive oxygen species production and pH during mechanosensing in Arabidopsis roots. *Plant Cell* 21:2341-56
127. Monshausen GB, Messerli MA, Gilroy S. 2008. Imaging of the Yellow Cameleon 3.6 indicator reveals that elevations in cytosolic Ca2+ follow oscillating increases in growth in root hairs of Arabidopsis. *Plant Physiol* 147:1690-8
128. Monshausen GB, Miller ND, Murphy AS, Gilroy S. 2011. Dynamics of auxin-dependent Ca2+ and pH signaling in root growth revealed by integrating high-resolution imaging with automated computer vision-based analysis. *Plant J* 65:309-18
129. Mori IC, Murata Y, Yang Y, Munemasa S, Wang YF, et al. 2006. CDPKs CPK6 and CPK3 function in ABA regulation of guard cell S-type anion- and Ca(2+)-permeable channels and stomatal closure. *PLoS Biol* 4:e327
130. Moseyko N, Feldman LJ. 2001. Expression of pH-sensitive green fluorescent protein in Arabidopsis thaliana. *Plant Cell Environ* 24:557-63
131. Mukherjee P, Banerjee S, Wheeler A, Ratliff LA, Irigoyen S, et al. 2015. Live imaging of inorganic phosphate in plants with cellular and subcellular resolution. *Plant Physiol* 167:628-38
132. Muller B, Fastner A, Karmann J, Mansch V, Hoffmann T, et al. 2015. Amino Acid Export in Developing Arabidopsis Seeds Depends on UmamiT Facilitators. *Curr Biol* 25:3126-31
133. Muller B, Sheen J. 2008. Cytokinin and auxin interaction in root stem-cell specification during early embryogenesis. *Nature* 453:1094-7
134. Munemasa S, Oda K, Watanabe-Sugimoto M, Nakamura Y, Shimoishi Y, Murata Y. 2007. The coronatine-insensitive 1 mutation reveals the hormonal signaling interaction between abscisic acid and methyl jasmonate in Arabidopsis guard cells. Specific impairment of ion channel activation and second messenger production. *Plant Physiol* 143:1398-407
135. Munnik T, Testerink C. 2009. Plant phospholipid signaling: "in a nutshell". *J Lipid Res* 50 Suppl:S260-5
136. Murase K, Hirano Y, Sun TP, Hakoshima T. 2008. Gibberellin-induced DELLA recognition by the gibberellin receptor GID1. *Nature* 456:459-63
137. Nadler DC, Morgan SA, Flamholz A, Kortright KE, Savage DF. 2016. Rapid construction of metabolite biosensors using domain-insertion profiling. *Nat Commun* 7:12266
138. Nagai T, Sawano A, Park ES, Miyawaki A. 2001. Circularly permuted green fluorescent proteins engineered to sense Ca2+. *Proc Natl Acad Sci U S A* 98:3197-202
139. Nagai T, Yamada S, Tominaga T, Ichikawa M, Miyawaki A. 2004. Expanded dynamic range of fluorescent indicators for Ca(2+) by circularly permuted yellow fluorescent proteins. *Proc Natl Acad Sci U S A* 101:10554-9
140. Nakai J, Ohkura M, Imoto K. 2001. A high signal-to-noise Ca(2+) probe composed of a single green fluorescent protein. *Nat Biotechnol* 19:137-41

141. Ngo QA, Vogler H, Lituiev DS, Nestorova A, Grossniklaus U. 2014. A calcium dialog mediated by the FERONIA signal transduction pathway controls plant sperm delivery. *Dev Cell* 29:491-500
142. Novak O, Napier R, Ljung K. 2017. Zooming In on Plant Hormone Analysis: Tissue- and Cell-Specific Approaches. *Annu Rev Plant Biol* 68:323-48
143. O'Connor N, Silver RB. 2007. Ratio imaging: practical considerations for measuring intracellular Ca2+ and pH in living cells. *Methods Cell Biol* 81:415-33
144. Okumoto S, Jones A, Frommer WB. 2012. Quantitative imaging with fluorescent biosensors. *Annu Rev Plant Biol* 63:663-706
145. Oldroyd GE. 2013. Speak, friend, and enter: signalling systems that promote beneficial symbiotic associations in plants. *Nat Rev Microbiol* 11:252-63
146. Ostergaard H, Henriksen A, Hansen FG, Winther JR. 2001. Shedding light on disulfide bond formation: engineering a redox switch in green fluorescent protein. *EMBO J* 20:5853-62
147. Ottenschlager I, Wolff P, Wolverton C, Bhalerao RP, Sandberg G, et al. 2003. Gravity-regulated differential auxin transport from columella to lateral root cap cells. *Proc Natl Acad Sci U S A* 100:2987-91
148. Palmer AE, Giacomello M, Kortemme T, Hires SA, Lev-Ram V, et al. 2006. Ca2+ indicators based on computationally redesigned calmodulin-peptide pairs. *Chem Biol* 13:521-30
149. Parton RM, Fischer-Parton S, Trewavas AJ, Watahiki MK. 2003. Pollen tubes exhibit regular periodic membrane trafficking events in the absence of apical extension. *J Cell Sci* 116:2707-19
150. Pei ZM, Murata Y, Benning G, Thomine S, Klusener B, et al. 2000. Calcium channels activated by hydrogen peroxide mediate abscisic acid signalling in guard cells. *Nature* 406:731-4
151. Perez Koldenkova V, Nagai T. 2013. Genetically encoded Ca(2+) indicators: properties and evaluation. *Biochim Biophys Acta* 1833:1787-97
152. Peroza EA, Boumezbeur AH, Zamboni N. 2015. Rapid, randomized development of genetically encoded FRET sensors for small molecules. *Analyst* 140:4540-8
153. Persechini A, Lynch JA, Romoser VA. 1997. Novel fluorescent indicator proteins for monitoring free intracellular Ca2+. *Cell Calcium* 22:209-16
154. Procko C, Burko Y, Jaillais Y, Ljung K, Long JA, Chory J. 2016. The epidermis coordinates auxin-induced stem growth in response to shade. *Genes Dev* 30:1529-41
155. Richmond TA, Takahashi TT, Shimkhada R, Bernsdorf J. 2000. Engineered metal binding sites on green fluorescence protein. *Biochem Biophys Res Commun* 268:462-5
156. Rincon-Zachary M, Teaster ND, Sparks JA, Valster AH, Motes CM, Blancaflor EB. 2010. Fluorescence resonance energy transfer-sensitized emission of yellow cameleon 3.60 reveals root zone-specific calcium signatures in Arabidopsis in response to aluminum and other trivalent cations. *Plant Physiol* 152:1442-58
157. Rosa S, De Lucia F, Mylne JS, Zhu D, Ohmido N, et al. 2013. Physical clustering of FLC alleles during Polycomb-mediated epigenetic silencing in vernalization. *Genes Dev* 27:1845-50
158. Rose T, Goltstein PM, Portugues R, Griesbeck O. 2014. Putting a finishing touch on GECIs. *Front Mol Neurosci* 7:88
159. Rosenwasser S, Rot I, Meyer AJ, Feldman L, Jiang K, Friedman H. 2010. A fluorometer-based method for monitoring oxidation of redox-sensitive GFP (roGFP) during development and extended dark stress. *Physiol Plant* 138:493-502
160. Sabatini S, Beis D, Wolkenfelt H, Murfett J, Guilfoyle T, et al. 1999. An auxin-dependent distal organizer of pattern and polarity in the Arabidopsis root. *Cell* 99:463-72
161. Sadanandom A, Napier RM. 2010. Biosensors in plants. *Curr Opin Plant Biol* 13:736-43
162. Samodelov SL, Beyer HM, Guo X, Augustin M, Jia KP, et al. 2016. StrigoQuant: A genetically encoded biosensor for quantifying strigolactone activity and specificity. *Sci Adv* 2:e1601266

163. Sato EM, Hijazi H, Bennett MJ, Vissenberg K, Swarup R. 2015. New insights into root gravitropic signalling. *J Exp Bot* 66:2155-65
164. Sauret-Gueto S, Calder G, Harberd NP. 2012. Transient gibberellin application promotes Arabidopsis thaliana hypocotyl cell elongation without maintaining transverse orientation of microtubules on the outer tangential wall of epidermal cells. *Plant J* 69:628-39
165. Schulte A, Lorenzen I, Bottcher M, Plieth C. 2006. A novel fluorescent pH probe for expression in plants. *Plant Methods* 2:7
166. Schumacher K. 2014. pH in the plant endomembrane system-an import and export business. *Curr Opin Plant Biol* 22:71-6
167. Schumacher K, Vafeados D, McCarthy M, Sze H, Wilkins T, Chory J. 1999. The Arabidopsis det3 mutant reveals a central role for the vacuolar H(+)-ATPase in plant growth and development. *Genes Dev* 13:3259-70
168. Schwarzlander M, Fricker MD, Muller C, Marty L, Brach T, et al. 2008. Confocal imaging of glutathione redox potential in living plant cells. *J Microsc* 231:299-316
169. Shaner NC, Patterson GH, Davidson MW. 2007. Advances in fluorescent protein technology. *J Cell Sci* 120:4247-60
170. Shaner NC, Steinbach PA, Tsien RY. 2005. A guide to choosing fluorescent proteins. *Nat Methods* 2:905-9
171. Shen J, Zeng Y, Zhuang X, Sun L, Yao X, et al. 2013. Organelle pH in the Arabidopsis endomembrane system. *Mol Plant* 6:1419-37
172. Shih HW, DePew CL, Miller ND, Monshausen GB. 2015. The Cyclic Nucleotide-Gated Channel CNGC14 Regulates Root Gravitropism in Arabidopsis thaliana. *Curr Biol* 25:3119-25
173. Sieberer BJ, Chabaud M, Fournier J, Timmers AC, Barker DG. 2012. A switch in Ca2+ spiking signature is concomitant with endosymbiotic microbe entry into cortical root cells of Medicago truncatula. *Plant J* 69:822-30
174. Sieberer BJ, Chabaud M, Timmers AC, Monin A, Fournier J, Barker DG. 2009. A nuclear-targeted cameleon demonstrates intranuclear Ca2+ spiking in Medicago truncatula root hairs in response to rhizobial nodulation factors. *Plant Physiol* 151:1197-206
175. Silverstone AL, Tseng TS, Swain SM, Dill A, Jeong SY, et al. 2007. Functional analysis of SPINDLY in gibberellin signaling in Arabidopsis. *Plant Physiol* 143:987-1000
176. Simon ML, Platre MP, Assil S, van Wijk R, Chen WY, et al. 2014. A multi-colour/multi-affinity marker set to visualize phosphoinositide dynamics in Arabidopsis. *Plant J* 77:322-37
177. Sozzani R, Busch W, Spalding EP, Benfey PN. 2014. Advanced imaging techniques for the study of plant growth and development. *Trends Plant Sci* 19:304-10
178. Steinhorst L, Kudla J. 2013. Calcium - a central regulator of pollen germination and tube growth. *Biochim Biophys Acta* 1833:1573-81
179. Stepanova AN, Yun J, Likhacheva AV, Alonso JM. 2007. Multilevel interactions between ethylene and auxin in Arabidopsis roots. *Plant Cell* 19:2169-85
180. Suzuki J, Kanemaru K, Ishii K, Ohkura M, Okubo Y, Iino M. 2014. Imaging intraorganellar Ca2+ at subcellular resolution using CEPIA. *Nat Commun* 5:4153
181. Swarup K, Benkova E, Swarup R, Casimiro I, Peret B, et al. 2008. The auxin influx carrier LAX3 promotes lateral root emergence. *Nat Cell Biol* 10:946-54
182. Tang S, Wong HC, Wang ZM, Huang Y, Zou J, et al. 2011. Design and application of a class of sensors to monitor Ca2+ dynamics in high Ca2+ concentration cellular compartments. *Proc Natl Acad Sci U S A* 108:16265-70
183. Thestrup T, Litzlbauer J, Bartholomaus I, Mues M, Russo L, et al. 2014. Optimized ratiometric calcium sensors for functional in vivo imaging of neurons and T lymphocytes. *Nat Methods* 11:175-82

184. Thor K, Peiter E. 2014. Cytosolic calcium signals elicited by the pathogen-associated molecular pattern flg22 in stomatal guard cells are of an oscillatory nature. *New Phytol* 204:873-81
185. Tian L, Hires SA, Mao T, Huber D, Chiappe ME, et al. 2009. Imaging neural activity in worms, flies and mice with improved GCaMP calcium indicators. *Nat Methods* 6:875-81
186. Ulmasov T, Murfett J, Hagen G, Guilfoyle TJ. 1997. Aux/IAA proteins repress expression of reporter genes containing natural and highly active synthetic auxin response elements. *Plant Cell* 9:1963-71
187. Uslu VV, Grossmann G. 2016. The biosensor toolbox for plant developmental biology. *Curr Opin Plant Biol* 29:138-47
188. Vermeer JE, Munnik T. 2013. Using genetically encoded fluorescent reporters to image lipid signalling in living plants. *Methods Mol Biol* 1009:283-9
189. Vermeer JE, Thole JM, Goedhart J, Nielsen E, Munnik T, Gadella TW, Jr. 2009. Imaging phosphatidylinositol 4-phosphate dynamics in living plant cells. *Plant J* 57:356-72
190. Vinkenborg JL, Nicolson TJ, Bellomo EA, Koay MS, Rutter GA, Merkx M. 2009. Genetically encoded FRET sensors to monitor intracellular Zn2+ homeostasis. *Nat Methods* 6:737-40
191. von Wiren N, Gazzarrini S, Gojon A, Frommer WB. 2000. The molecular physiology of ammonium uptake and retrieval. *Curr Opin Plant Biol* 3:254-61
192. Waadt R, Hitomi K, Nishimura N, Hitomi C, Adams SR, et al. 2014. FRET-based reporters for the direct visualization of abscisic acid concentration changes and distribution in Arabidopsis. *Elife* 3:e01739
193. Waadt R, Hsu PK, Schroeder JI. 2015. Abscisic acid and other plant hormones: Methods to visualize distribution and signaling. *Bioessays* 37:1338-49
194. Wachter RM, Remington SJ. 1999. Sensitivity of the yellow variant of green fluorescent protein to halides and nitrate. *Curr Biol* 9:R628-9
195. Wagner S, Behera S, De Bortoli S, Logan DC, Fuchs P, et al. 2015. The EF-Hand Ca2+ Binding Protein MICU Choreographs Mitochondrial Ca2+ Dynamics in Arabidopsis. *Plant Cell* 27:3190-212
196. Wang YF, Munemasa S, Nishimura N, Ren HM, Robert N, et al. 2013. Identification of cyclic GMP-activated nonselective Ca2+-permeable cation channels and associated CNGC5 and CNGC6 genes in Arabidopsis guard cells. *Plant Physiol* 163:578-90
197. Weinl S, Held K, Schlucking K, Steinhorst L, Kuhlgert S, et al. 2008. A plastid protein crucial for Ca2+-regulated stomatal responses. *New Phytol* 179:675-86
198. Wells DM, Laplaze L, Bennett MJ, Vernoux T. 2013. Biosensors for phytohormone quantification: challenges, solutions, and opportunities. *Trends Plant Sci* 18:244-9
199. Wrzaczek M, Brosche M, Kangasjarvi J. 2013. ROS signaling loops - production, perception, regulation. *Curr Opin Plant Biol* 16:575-82
200. Xue S, Hu H, Ries A, Merilo E, Kollist H, Schroeder JI. 2011. Central functions of bicarbonate in S-type anion channel activation and OST1 protein kinase in CO2 signal transduction in guard cell. *EMBO J* 30:1645-58
201. Yang H, Bogner M, Stierhof YD, Ludewig U. 2010. H-independent glutamine transport in plant root tips. *PLoS One* 5:e8917
202. Ye W, Muroyama D, Munemasa S, Nakamura Y, Mori IC, Murata Y. 2013. Calcium-dependent protein kinase CPK6 positively functions in induction by yeast elicitor of stomatal closure and inhibition by yeast elicitor of light-induced stomatal opening in Arabidopsis. *Plant Physiol* 163:591-9
203. Young JJ, Mehta S, Israelsson M, Godoski J, Grill E, Schroeder JI. 2006. CO(2) signaling in guard cells: calcium sensitivity response modulation, a Ca(2+)-independent phase, and CO(2) insensitivity of the gca2 mutant. *Proc Natl Acad Sci U S A* 103:7506-11

204. Yuan F, Yang H, Xue Y, Kong D, Ye R, et al. 2014. OSCA1 mediates osmotic-stress-evoked Ca2+ increases vital for osmosensing in Arabidopsis. *Nature* 514:367-71
205. Zhao Y, Araki S, Wu J, Teramoto T, Chang YF, et al. 2011. An expanded palette of genetically encoded Ca(2)(+) indicators. *Science* 333:1888-91
206. Zhu Q, Wang L, Dong Q, Chang S, Wen K, et al. 2017. FRET-based glucose imaging identifies glucose signalling in response to biotic and abiotic stresses in rice roots. *J Plant Physiol* 215:65-72
207. Zurcher E, Tavor-Deslex D, Lituiev D, Enkerli K, Tarr PT, Muller B. 2013. A robust and sensitive synthetic sensor to monitor the transcriptional output of the cytokinin signaling network in planta. *Plant Physiol* 161:1066-75

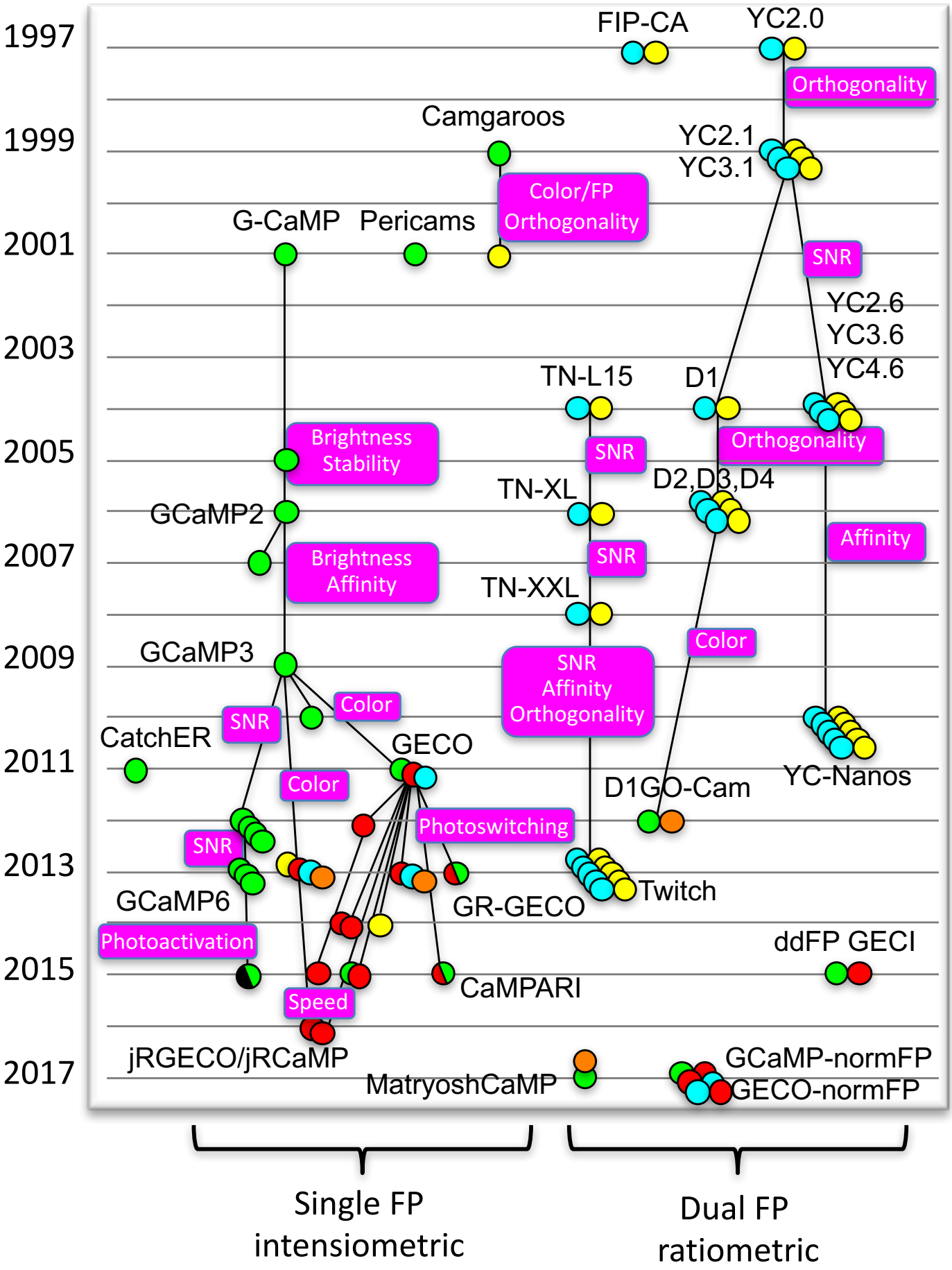

Figure 1. Twenty years of fluorescent GECIs. Evolution of genetically-encoded calcium indicators over the last 20 years with biosensors plotted as dots on the year of publication that are colored according to the emission wavelength of their constituent fluorophores. Single FP biosensors are plotted at left and double-FP biosensors at right.

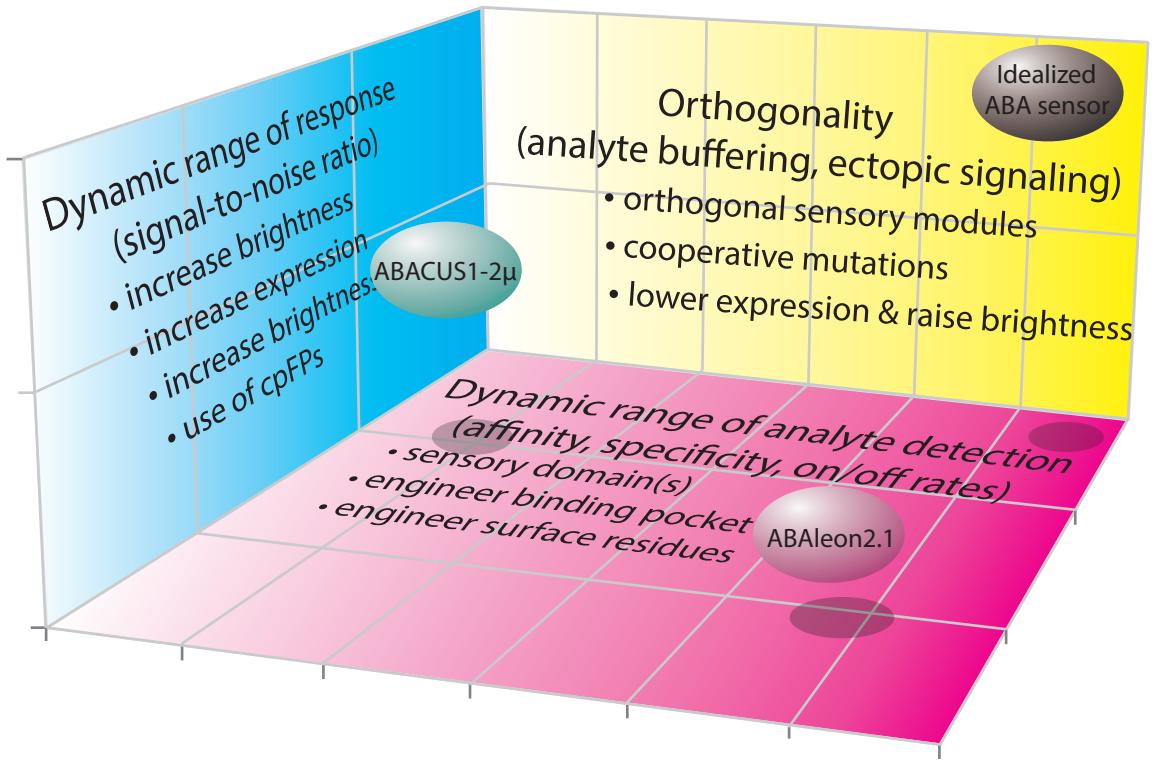

Further considerations

- Color (imaging, autofluorescence, multiplexing)
- Brightness
- Expression in vivo (silencing, cell-types)
- Subcellular localization
- Intensiometric vs ratiometric
- In vivo control sensors
- Imaging modality
- Image analysis

Figure 2. Biosensor considerations. The successful engineering and use of genetically encoded biosensors relies on appropriate consideration of the key parameters diagrammed. To offer an example, the contrasting features and limitations of current ABA biosensors [ABACUS1-2µ and ABAleon2.1 (89; 192)] as well as a idealized ABA biosensors are plotted. An idealised biosensor should display high dynamic range of biosensor response, a dynamic range of analyte detection that is physiologically relevant, as well as high orthogonality.

a

Agar/vaccuum grease chamber

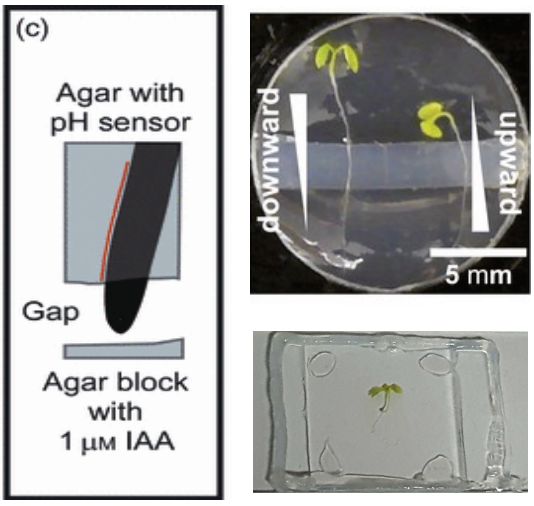

b

Treatment chambers (adhesive restraint)

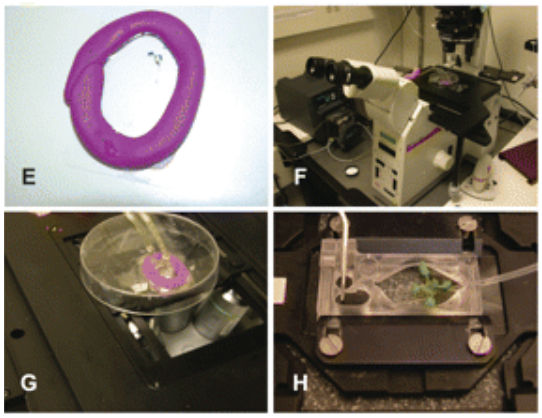

c

Perfusion chambers (mechanical restraint)

Custom-built

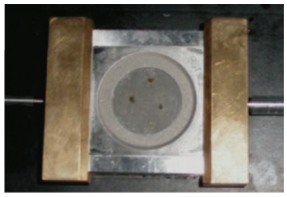

Commercial

SecureSeal

IBIDI slides

d

Microfluidics perfusion chambers

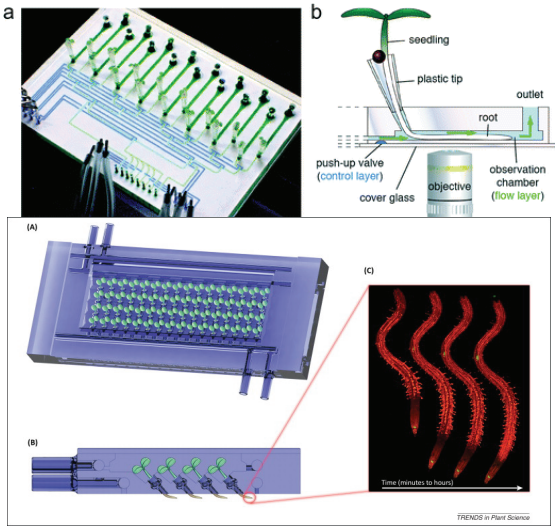

Figure 3. Biosensor imaging modalities. Schematic illustrations to show various imaging modalities for plants expressing biosensors (Currently presented as photos, suggest to convert to schematics/diagrams with the assistance of ARPB artists). (a) Agar- or vacuum grease-based approaches to monitor biosensor responses to short-term experimental treatments (128; 192), (Rizza et al, in press), (b) Chambers using adhesive restraint to monitor biosensor response to short-term treatments (35), (c) Perfusion based chambers using mechanical restraint to monitor biosensor responses (long-term or short-term) to various treatments using custom-built chambers (99; 164), IBIDI slides (37), and SecureSealTM (157), (d) Microfluidics-based perfusion chambers to monitor biosensor responses (long-term or short-term) in plant roots (67; 177).

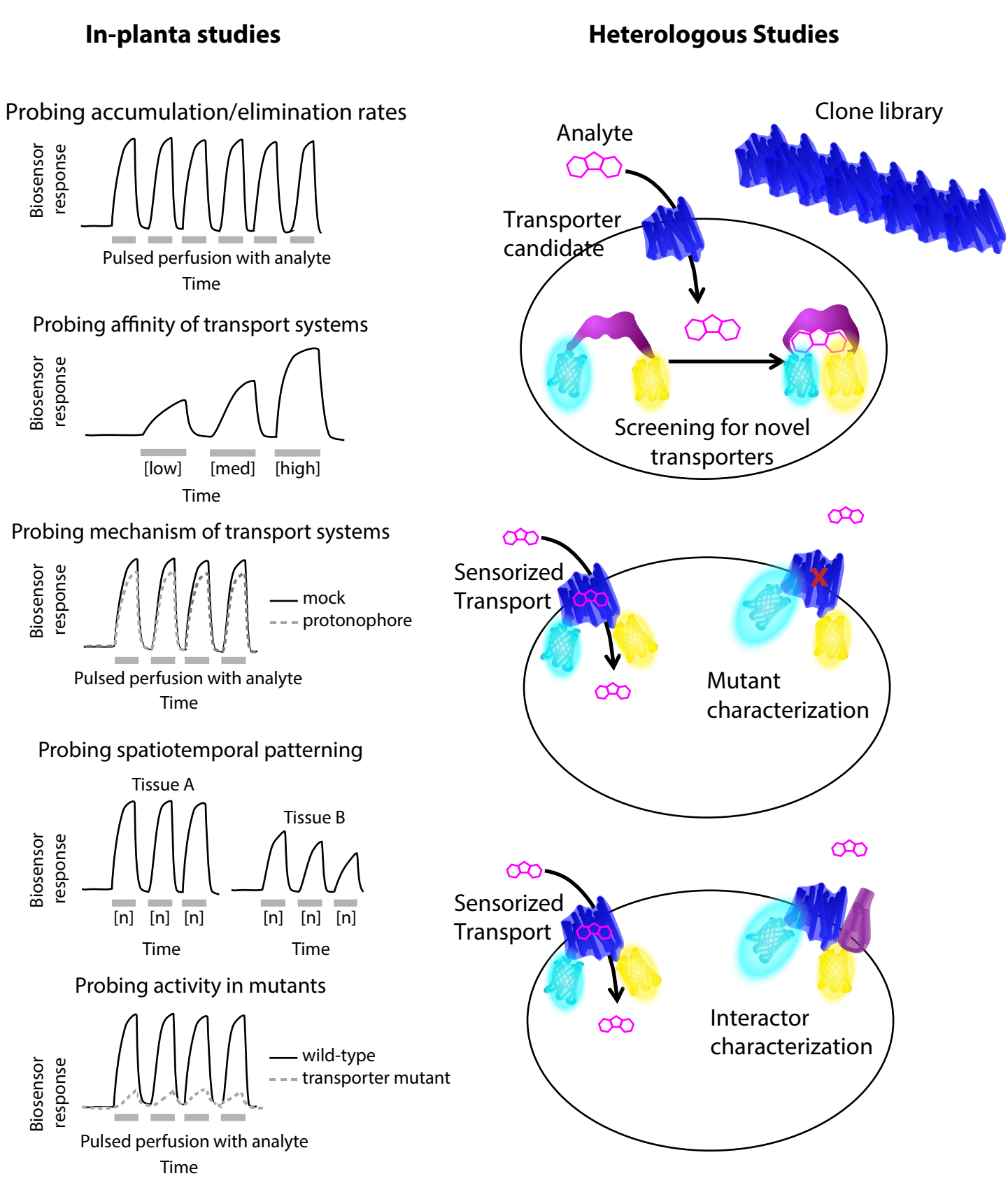

Figure 4. Biosensors for studying transport. (Left) Genetically encoded biosensors have been used in planta to monitor accumulation and elimination rates of during and following pulsed application of exogenous analytes (e.g. (48)). This approach allows the interrogation of transport activities in vivo and can be applied to indirectly probe affinity (e.g. (89)), mechanisms (e.g. (36)), and spatiotemporal patterning (e.g. Rizza et al. In press) of transport activities. Also, such analyses can reveal quantitative molecular phenotypes in mutant lines expressing biosensors (e.g. (131)). (Right) Biosensors have also been used in heterologous systems to screen for novel plant transporters (e.g. SWEET1 (38)), and, through the use of sensorized transporters, to rapidly interrogate the effects of mutations and protein interactions on activity of plant transporters (e.g. NRT1.1/CHL1/NPF6.3 (78)).